This paper is a non-peer reviewed preprint submitted to *EarthArXiv*. The manuscript was submitted to *Nature Geoscience* for peer review. Future updates on this manuscript will be provided once it's peer-reviewed or accepted. Please feel free to contact me at: shiche@oregonstate.edu if you have any questions or feedbacks.

Soil Organic Matter Composition Improves Predictions of Potential Soil Respiration across the Continental United States

Cheng Shi (shiche@oregonstate.edu)[a], Maruti Mudunuru (maruti@pnnl.gov)[b], Maggie Bowman (maggie.bowman6@gmail.com)[c], Qian Zhao (qian.zhao@pnnl.gov)[c], Jason Toyoda (Jason.Toyoda@pnnl.gov)[c], William Kew (william.kew@pnnl.gov)[c], Yuri Corilo (corilo@pnnl.gov)[c], Odeta Qafoku (Odeta.Qafoku@pnnl.gov)[c], John R. Bargar (john.bargar@pnnl.gov)[c], Satish Karra (karra@pnnl.gov)[c], & Emily Graham (emily.graham@pnnl.gov)[d,e*]

[a]Oregon State University, Department of Biological & Ecological Engineering, Corvallis, OR, United States.
[b]Energy and Environment Directorate, Pacific Northwest National Laboratory, Richland, WA, United States.
[c] Environmental Molecular Science Laboratory, Pacific Northwest National Laboratory, Richland, WA, United States.
[d]Earth and Biological Sciences Directorate, Pacific Northwest National Laboratory, Richland, WA, United States.
[e]School of Biological Sciences, Washington State University, Pullman, WA, United States.
co

*Corresponding author: emily.graham@pnnl.gov
Twitter handle: @mpchengsworld, @emilybonnell_g, @EMSLscience

Abstract

Despite the importance of microbial respiration of soil organic matter (SOM) in regulating carbon flux between soils and the atmosphere, soil carbon (C) cycling models remain primarily based on climate and soil properties, leading to large uncertainty in their predictions. Molecular data have long been proposed as a promising avenue for resolving modeling errors, but evidence for improved predictions of soil C cycles with high-resolution measurements remains mixed. With data from the 1000 Soils Pilot of the Molecular Observation Network (MONet), we analyzed the molecular composition of water-extractable SOM from 66 soil cores across the United States to address this knowledge gap. Our innovation lies in using machine learning (ML) to distill the thousands of SOM formula that we detected per sample into tractable units. Then, we compared ML predictions of measured potential soil respiration using (1) a suite of standard soil physicochemical data, (2) ultrahigh-resolution SOM composition independently, and (3) in combination with physicochemistry to assess the added value of molecular information to predict soil respiration. In surface soils (0-10 cm), water-extractable SOM chemistry alone provided better estimates of potential soil respiration than soil physicochemical factors alone, and using the combined sets of predictors yielded the highest explanatory power of soil respiration rates. In contrast, in subsoils (>10 cm), SOM composition did not improve ML-based respiration model performance, possibly due to the greater importance of mineral-associated SOM below the surface layer. Our results underscore a role of water-extractable SOM as a determinant of soil respiration and a need to integrate SOM composition into carbon cycle modeling for enhanced predictions of terrestrial-atmosphere climate feedback.

Introduction

Soil respiration is estimated to release 60-100 Gt of C to the atmosphere per year,[1, 2] six to ten times as much C as released by fossil fuel combustion (~10 Gt C[3]). Microbial respiration of soil organic matter (SOM) is one of the most important contributors to soil carbon dioxide (CO_2) emissions and a critical link in the global C cycle.[4] With increasing temperatures under climate change, soil C repositories are vulnerable to increased rates of microbial respiration,[5-7] which can lead to positive feedbacks in global CO_2 emissions and temperature rises.[8] Despite decades of research, soil C fluxes remain one of the largest uncertainties in global climate predictions.[9-14] Novel molecular measurements have recently been applied to identify SOM composition in an effort to understand molecular-scale processes that could improve model predictions of CO_2 fluxes.[15-18] Despite these efforts, our attempts to improve soil C model predictions by refining chemical pools have yielded mixed results.[19-21]

The interplay of factors such as soil moisture, pH, nutrients, mineralogy, and SOM concentration and chemistry governs microbially-derived transformations of SOM;[22-27] but these relationships are difficult to constrain.[4, 28] The most commonly used modeling approaches are based on Raich's model, which estimates respiration primarily as a function of temperature and water availability.[29, 30] Newer process-based model formulations use an additional suite of physical and biogeochemical measurements to represent microbial and mineral processes. They incorporate SOM chemistry either through several discrete pools or through their thermodynamic properties.[21, 31-34] With large spatiotemporal heterogeneity and limited availability of comprehensive and standardized measurements at regional-to-continental scales, accurate predictions of microbial SOM decomposition across different ecosystems remain challenging.[35]

A better understanding of SOM concentration, composition, and bioavailability may enhance our ability to predict soil C cycling processes through their controls on soil respiration and related enzymatic activities.[21, 31-34] Variations in the bioavailability of chemical classes of SOM are mediated by geochemical conditions and biophysical constraints, such as microbial biomass and necromass, reactive metals and minerals, organic and mineral horizon thickness, and other climate-related variables.[36] For example, coarse-textured soil is more conducive to decomposition of chemically labile litter-derived C potentially due to higher fungal activity in

organic-rich horizons.[37, 38] In addition, the interface between fresh litter inputs and soil minerals can serve as a hotspot for microbial breakdown of C found in the litter, resulting in the formation of soil aggregates and organo-mineral associations.[39] This variability underlines the essential need to identify unique subsets of SOM formula that contribute more to soil respiration among different ecosystems and soil depths.

The distillation of multidimensional SOM composition profiles into a tractable set of formula that influence soil respiration is a key challenge in soil ecology.[15, 28, 40-45] Unsupervised machine learning models that summarize large data into a small number of significant features have been widely used to study microbial communities, SOM composition, and other environmental problems with multidimensional data.[46] Dimensionality reduction such as principal component analysis (PCA)[47-49] and clustering methods such as hierarchical clustering analysis[50-52] are the most common tools to explore large molecular datasets. Although these tools are beginning to be applied to determine the relationship between SOM composition and soil physicochemistry,[49] it is still challenging to extract a subset of SOM features associated with specific processes, like soil respiration.

Although ultrahigh mass resolution measurements can provide unprecedented characterization of the thousands of individual formulae that comprise SOM, the interpretation of these data types largely remains guided by coarse chemical and ecological groupings. Here, we develop models using semi-supervised machine learning (non-negative matrix factorization with custom *k*-means clustering, NMF*k*) to reduce the complexity of molecular information into *k* distinct signatures of water-extractable SOM chemistry at two depths in cores collected across the continental United States. We then explore the extent to which these signatures and NMF*k*-enabled feature set can provide additional insight into rates of soil respiration beyond variables that are more routinely collected. By examining a multitude of physicochemical and SOM factors, our goal is to elucidate the specific aspects of SOM chemistry that may be vital to understanding and predicting below-ground C storage.

Methods

Soil sampling and characterization.

As part of the 1000 Soils Pilot study for the Molecular Observation Network (MONet) program, we collected 66 soils from across the continental US using standardized sampling procedures described by Bowman et al.[53] (Figure S1). Two long cores (30 cm) and three short cores (10 cm) were collected at each site. We also conducted field measurements, including soil temperature, volumetric water content, vegetation type, and weather conditions. Cores were shipped on ice overnight to the Pacific Northwest Laboratory for further analysis. A full description of sampling and analytical methodologies is available in Bowman et al.[53]

Briefly, once soil cores were delivered to the lab, we divided the 30-cm cores into 10 cm depth intervals, where only the top (hereafter, surface or surficial soil) and bottom (hereafter, subsoil) sections were used for further analysis. We mixed the top sections with three short cores to homogenize the local variation. The soils were then sieved through 4 mm sieves separately to remove rocks and root structures. We measured gravimetric water content (GWC) by drying 10 g of soil for 24 hours in a drying oven at 100 ºC. We measured soil pH by mixing 20 g of dry soil with 20 mL of DI water (1000 rpm on reciprocating shaker for 15 minutes), and tested with a calibrated pH probe. Soil microbial biomass C and nitrogen (N) content were measured via chloroform fumigation.[54-56] We extracted phosphorus contents using Bray (pH < 7) or Olsen extractions (pH > 7),[57, 58] and extracted nitrate and ammonium with 0.5M K_2SO_4 and tested by colorimetric methods. Ion concentrations of potassium (K), calcium (Ca), magnesium (Mg), and sodium (Na) from 1:10 ammonium acetate extraction, Zinc (Zn), manganese (Mn), copper (Cu), iron (Fe), boron (B), and sulfate (SO_4^{2-}) from 1:2 soil to diethylenetriaminepentaacetic acid (DPTA) extraction were measured using Inductively coupled plasma mass spectrometry (ICP-MS). We measured total C and N using the AOAC official methods 972.43.[59] Soil texture was measured by hydrometer analysis. Finally, we assessed potential soil respiration using the CO_2 burst method with 24 hours of incubation at 24 ºC.[53]

Water extractable SOM characterization.

We extracted water-soluble SOM by mixing 6 g of dry soil with 30 ml DI water in triplicates, shaken for 2 hours at 800 rpm, and centrifuged at 6,000 rpm for 8 minutes. 5 ml of supernatant was acidified with 2 µl concentrated phosphoric acid (37%), and then loaded onto Agilent Bond Elut PPL solid phase extraction (SPE) cartridges[60] with Gilson ASPEC® SPE system. A Bruker 7 T Fourier transform ion cyclotron resonance mass spectrometry (FTICR MS) at the Environmental Molecular Sciences Laboratory (EMSL) in Richland, WA, was used to analyze SOM composition, with a negative ionization mode and ion accumulation time at 0.01 or 0.025 seconds (depending on dissolved organic C concentration). The measured mass accuracy was typically within 1 ppm. One lab blank and one Suwannee River Fulvic Acid (SRFA) sample (20 ppm) were tested every 30 soils to evaluate instrument performance.

Raw FTICR MS data was processed with CoreMS (Python package, installed on 2022/11/22),[61] including signal processing, peak detection, and molecular formula assignment. Noise thresholding was performed with signal-to-noise threshold (5 std.), mass error (0.3 ppm), and stoichiometric limits from domain knowledge (supporting information). Suwannee River fulvic acid (SRFA) standards were used to set a calibration threshold for all soils in the same batch. Molecular formula was assigned based on both accurate mass and filtered by their confidence score from CoreMS. After calibration and formulae assignment, we filtered the assigned peaks by *m/z* between 200 to 1,000, present in at least 2 out of 3 replicates, not present in two or more lab blanks, and with formulae confidence scores (combines *m/z* error and isotopic pattern)[61] above 0.7. We predicted compound classes of the filtered formulae based on O/C and H/C ratios of van Krevelen classes.[62, 63] The suffix "-like" in chemical classes indicates the uncertainty of the van Krevelen classification method.[63] We converted the peak intensity values to present/absent (1/0) and separated the final dataset by soil depth (surface vs. subsoil) for statistical analysis. Alpha diversity was calculated as the total number of SOM formulae identified in each sample.

Data analysis and machine learning methods.

We used linear regression models to evaluate the relationship between soil potential respiration and soil physicochemical variables. To avoid the impacts of different magnitudes of the data that

might lead to biased relationships, we performed $\log_{10}$ transformation on potential respiration rates, total C, total N, total sulfur, and Mn concentration. *stats.linregress* function from *scipy* package (v 1.11.4) in Python (v 3.7.1) was applied to calculate the fitted line, r^2 value (*rvalue*^{2}, Pearson correlation), and p-value (*pvalue*). Pairwise plots with regression fitting were generated by the pairplot function from the *seaborn* package (v 0.12.1) in Python.

We used non-negative matrix factorization (NMF)[64] with custom k-means clustering (NMF*k*)[65] to identify signature components from the 7,312 and 5,515 SOM molecular formula (for surface and subsoil, respectively) we detected (i.e., *N* formulae in *m* soils) with *pyNMFk* package (Python, https://github.com/lanl/pyDNMFk, Figure 1). More details on NMF*k* assumptions, model settings, and model robustness are in the supporting information. Briefly, NMF*k* tends to be more successful at extracting explainable basis or signatures from large multivariate datasets, compared to other dimensionality reduction tools such as principal component analysis.[64, 66] As applied here, NMF*k* summarizes data into discrete signatures that contain weights for each SOM formulae detected by FTICR-MS for each soil layer independently (i.e., a separate set of signatures was generated to summarize surface versus subsoils, allowing us to explore depth-specific relationships with potential soil respiration). The optimal number of signatures was determined from silhouette coefficients of different NMF*k* models. A W-matrix with the weights of each SOM formulae (*N*) to each extracted signature (*k*), and an H-matrix with the contribution of each signature (*k*) to each soil sample (*m*) were generated from NMF*k*. To visualize the composition of each NMF*k* signatures (W-matrix), we generated a heatmap of SOM formula with normalized weights (0-1) >0.5 in at least one NMF*k*, clustered by van Krevelen class assignment (clustermap function from seaborn package). Within each inferred chemical class of SOM formula, we further clustered formula using the "linkage" method from the *scipy* package ("ward" method with "Euclidean" distance) to illustrate the difference between NMF*k* signatures.

To define groups of soils with high, medium, or low rates of potential respiration, we used *k*-means clustering on potential soil respiration with the elbow method to select the number of groups (*KMeans* from *scikit-learn* package).[67]

Then, we mapped the extracted k signatures to soil respiration using supervised machine learning. To evaluate the potential value of NMF*k*-extracted SOM signatures for explaining soil respiration, we conducted three sets of machine learning models: (1) selected environmental parameters alone (i.e., variables with R^2 >0.2 in individual regressions, Figure 2, Table S1), (2) SOM composition alone (NMF*k* weights from H-matrix), and (3) environmental and SOM composition in combination. All machine learning models were built using gradient boosting regression (GBR) from *scikit-learn* package (v. 0.24, Python). Model hyperparameters were tuned first with 5-fold cross validation on 80% of each dataset (*train_test_split* in scikit-learn, with the same *random_state* for models in the same layer) using *RandomizedSearchCV* function from scikit-learn. We then used the best-tuned parameters with 80% of soils to build the finalized model. Root means square error (RMSE) was used to evaluate the error of models. More details on hyperparameter grids can be found in supporting information. All the models were then tested with the other 20% of soils to compare their performance. The most important predictors for the models with the best performance were then determined using MDI importance and/or mean decrease in impurity to infer potential relationships between soil environmental parameters, SOM composition, and potential soil respiration. Partial dependence plots were used to evaluate the response of potential respiration to the selected important features.

Results

Soil physicochemistry and potential respiration

Overall, many soil parameters, including potential soil respiration, tended to be higher in surface soils than in subsoils. Significant differences ($p<0.05$) between surface soils and subsoils in total C, total N, total sulfur, C/N ratio, and other factors are shown Figure S3. In particular, surface soils had higher potential respiration rates (median: 72.6 ug CO_2/g soil/day) than subsoils (median: 21.9 ug CO_2/g soil/day) (Mann–Whitney U = 3022.5, $N_{surface}$ = 63, $N_{subsoil}$ = 61, $P < 0.05$).

We grouped potential soil respiration into 3 levels corresponding to low, medium, and high respiration in each soil layer using k-means clustering (Figure S2). For both surface and subsoils, soil with high potential respiration tended to be sourced from the Midwestern and Northeastern

United States. (Figure 3, Figure S5). In surface soil, high potential respiration was associated with five soils collected in Utah, Wyoming, and Virginia (within temperate conifer forest and temperate broadleaf & mixed forest biomes, Figure 3, Figure S1). In subsoils, high respiration was associated with three soils from Utah and Maryland (temperate conifer forests and broadleaf & mixed forests biomes). Desert soils had the lowest respiration in both layers (Figure S1).

We found relationships between soil respiration and many variables that supported prevailing paradigms. A full correlation table of associations between different soil properties is available in the SI (Table S1). Briefly, potential respiration rates in both surface and subsoils were positively correlated with gravimetric water content (GWC) (r^2: 0.246 and 0.225, $p<0.05$) and cation exchange capacity (CEC, r^2: 0.405 and 0.354, $p<0.05$, Figure 2). They were also positively correlated with total C and total N content, with stronger relationships in surface soils (r^2: 0.487 v.s. 0.268 for total C, r^2: 0.439 v.s. 0.248 for total N, $p<0.05$). Total bases and magnesium (Mg) concentrations had a higher correlation to respiration in subsoils than surface soils (r^2: 0.227 v.s. 0.146 and 0.287 v.s. 0.160, $p<0.05$, Figure 2), while manganese (Mn) concentrations were correlated to respiration in surface soils (r^2: 0.324, $p<0.05$, Figure 2).

SOM composition and NMFk partitioning of SOM.

Across all soils, the most common chemical classes of SOM were lignin-, condensed hydrocarbon-, and tannin-like formula. Most formula in these classes were present in both surface and subsoils (i.e., ‘shared’ formula). However, surface soils contained more unique formula than subsoils for all compound classes (Figure 3b). In particular, many protein-, amino sugar-, and lipid-like compounds were identified in surface soils only, with very few compounds in these classes being unique to subsoils. Because SOM consists of thousands of different compounds, we also used alpha diversity to represent the SOM richness per sample (Figure 3). Soils from the Midwestern U.S. and the West Coast had relatively higher alpha diversity than soils from other regions.

We used NMF*k* to summarize SOM composition into 7 and 5 NMF*k* signatures, respectively, for surface and subsoils (Figure 4). Geographic patterns in SOM signatures are displayed in Figure

S6-7, with more geographic clustering of NMFs in surface soils than in subsoils. For surface soils, NMF3 presented as the largest relative contributor to SOM composition in 20 soils across all biomes (i.e., highest weighting in H-matrix, hereafter, 'dominant signature', Figure S6). NMF2, NMF5, and NMF7 served as the dominant signature in at least 9 soils each. For subsoils, NMF5 was the dominant signature in 27 soils distributed across all biomes in the continental United States. NMF2 appeared to be the second dominant SOM signature in subsoils with the highest weights in 16 soils. There was no single NMF signature that could exclusively represent SOM composition of all sites in the same region for either surface or subsoils, suggesting that SOM composition at local sites is best summarized by a combination of multiple NMFs.

The most important formula contributing to the composition of each NMF (i.e., formula with normalized weights >0.5 in W-matrix) are shown in Figure 4a-b. For surface soils, NMF1, 4, 6, and 7 had a relatively higher number of important compounds identified as lignin-like. NMF6 and 7 had larger contributions of condensed hydrocarbon-like formula. NMF1 had higher contribution from protein-like and amino sugar-like compounds, while NMF3 and 5 had the lowest contribution from protein-like, amino sugar-like, and lipid-like compounds, suggesting their low microbial activities. NMF4 had the largest number of lipid-like compounds as important features. In subsoil samples, important formula for all NMFs tended to be classified as lignin-, tannin-, and/or condensed hydrocarbon-like. NMF1 and NMF5 had most important features identified as lignin-like and some tannin-like compounds. NMF2 had the largest fraction of condensed hydrocarbon-like compounds. NMF4 had larger contributions of protein-like and amino sugar-like formula (Figure S8).

We also compared if formula contributing to NMF signatures tended to be similar among surface and subsoils by assessing shared vs unique formula. NMF-selected formula (weights >0.5 in W-matrix) followed the same general patterns as the overall SOM pool but showed amplified relationships (Figure 4c). Most shared formula belonged to lignin-, tannin-, and/or condensed hydrocarbon-like chemical classes. Very few NMF-selected formula were unique to subsoils, with lipid-, amino sugar-, and especially protein-like important formula unique to surface soils.

We also observed differences in dominant NMF signatures across high-, medium-, and low-respiration soils, particularly in surface soils (Figure 4d-e). High respiration surface soils were characterized by five NMF signatures (1, 2, 3, 6, and 7), with the largest contribution from NMF6. Low respiration surface soils, in contrast, uniquely contained NMF5, and they did not have any contribution from NMF6. In subsoils, high respiration soils consisted of NMF 1, 2 and 4, while low respiration soils consisted of NMF1, 2, and 5. NMF5 had a larger contribution in low-respiration soils from both temperate forests and grasslands/shrublands. NMF5 had higher weights in low-respiration soils, and NMF3 and NMF4 had lower weights in low-respiration soils.

Relative importance of physicochemistry and SOM composition in potential soil respiration models

We developed gradient-boosting regression models to predict potential soil respiration with (1) physicochemical variables, (2) SOM composition represented by NMF signatures, and (3) both of them combined. Model performances are summarized in Table 1 and Figure 5.

Selected physicochemical variables (consisting of total C, total N, CEC, moisture, Mn (surface), total base (subsoil), and Mg (subsoil) concentration) had significant independent Pearson's correlation to respiration w/ $p < 0.05$ and $r^2 > 0.2$ (Table S1). Physicochemical variables predicted potential respiration rates in surface and subsoils equally well ($R^2 = 0.44$ and 0.43 respectively for testing data). In surface soils, total C, total N, and cation exchange capacity (CEC) were identified as the top 3 most important predictors, followed by Mn concentration and soil moisture (Figure 4). In subsoils, CEC, total N, and soil moisture were the most important predictor, and total C was the least important predictor (Figure S9).

Using SOM composition (NMF signatures) as predictors, we had better model performance in surface soils than in subsoils (testing $R^2 = 0.54$ vs. 0.08), and SOM composition alone predicted more slightly variation in potential respiration rates than physicochemical variables alone in surface soils (testing $R^2 = 0.54$ vs. 0.44), even when controlling for an equal number of

predictors (testing R^2 = 0.48 vs. 0.44). NMF3, NMF5, and NMF2 were the most important SOM composition variables for explaining soil respiration in surface soils (Figure 5).

When we combined both physicochemical variables and SOM composition into a single predictor set, we obtained better respiration model performance (R^2 = 0.62) compared to models with environmental variables or SOM composition in surface soils only. However, the model describing potential respiration rates in subsoil was worse (R^2 = 0.36) when compared to models based on physicochemical variables only. In surface soils, the 3 most important variables were the same as the physicochemical model (Figure 5). NMF6 was identified as the most important SOM variable, followed by NMF3, NMF2, and NMF5 (Figure 5). In subsoils, total N and Mg concentration were the most important variables, followed by NMF5, total C and CEC.

Discussion

Soil respiration and physicochemistry

Soil moisture, total C, and total N appeared to regulate soil respiration in both surface soil and subsoil, as evidenced by positive correlations of total C, N, and moisture with potential soil respiration (Figure 2). This is consistent with previous work describing relationships between these properties and soil respiration, as well as other factors that we observed to be correlated with respiration including pH and CEC.[33, 68-70] Soil physical properties (e.g, moisture and pore space connectivity) can constrain microbial access to SOM molecules and nutrients isolated in soil pore networks, thereby regulating microbial respiration of SOM.[22, 33, 71-73] Additionally, C and N can limit soil respiration through stoichiometric constraints on biomass production.[4, 74-76]

We propose that differences in potential respiration between surface and subsoil may be related to variation in soil C composition and stabilization mechanisms across soil layers. We observed a steeper correlation between total C and potential soil respiration in surface soils than in subsoils, despite similar slopes for relationships of N and moisture with respiration at both depths. While we anticipated that microbial respiration would decrease significantly with soil depth,[77] the change in the nature of the relationship between C and respiration suggests that differences in SOM composition or microbial access to C substrates could be associated with potential rates of

respiration. Surface soils are generally rich in relatively bioavailable water-extractable organic matter and contain higher proportions of microbial biomass in contrast to subsoils that are more mineral with lower pore space connectivity and larger pools of mineral-associated organic matter.[78] Given previously observed differences in SOM composition and soil structure, we hypothesize that factors including oxygen availability and alternative electron acceptors may influence heterotrophic respiration to a greater degree than soil C as depth increases.

We also found a suite of correlations between elements and potential soil respiration that may reflect the influence of vegetation across rooting profiles; however, associations between inorganic nutrients (NH4+, NO3-, PO43-) and respiration were conspicuously absent ($p>0.05$, Table S1).[79-82] Mg, Mn, Zn, and sulfate were correlated to potential soil respiration and are known to have strong impacts on plant productivity that provides chemically labile C sources for microbial respiration.[83-85] Mn can also influence soil respiration by regulating the activities of Mn peroxidase enzyme, a lignin-degrading enzyme produced by fungi and *Actinobacteria*.[86-90] Because total N corresponded to potential soil respiration, the lack of relationship between respiration and inorganic nutrients may indicate organic nutrients as key drivers of soil respiration. Alternatively, inorganic nutrient limitations that vary tremendously through space and time may not be observable across different ecosystems at the continental scale.[91, 92]

In additional to patterns in soil physicochemistry, we observed geographic patterns in potential soil respiration that contrasted with some previous estimates,[6] including high rates of potential soil respiration in the midwestern and mid-Atlantic regions, and at high elevations (Figure 3). A notable difference between Nissan et al. and the current study is that Nissan et al. report simulated mean annual values of heterotrophic respiration in soils, while the current study reports the measured potential respiration rates of sieved soils collected during the summer months. Because high latitude and high elevation ecosystems can exhibit intense, short-lived peaks of biomass during summertime,[93] soils collected during this period may have relatively extreme rates of potential respiration that are averaged out at the annual scale. Another interpretation for higher potential soil respiration at high elevation is that relative humidity typically increases with elevation and thus can stimulate higher microbial activities and SOM decomposition.[94] In contrast, comparatively low potential soil respiration recorded in the

Southeastern United States could also reflect the comparatively low C content of these soils that has been associated with faster turnover rates and high year-round temperatures.[95]

Depth partitioning in relationships between SOM composition and potential soil respiration

Differences in SOM composition with soil depth and across the continental United States were associated with potential soil respiration, supporting previous studies showing relationships between SOM composition and soil respiration rates (Figure 3).[8, 26, 27] Regardless of depth or geographic location, the diversity of water-extractable SOM compounds appeared to be a common factor in regulating potential soil respiration — soils with higher potential respiration generally had more diverse pools of water-extractable SOM (Figure 3d-e).

Our results were consistent with a paradigm in which chemically bioavailable, plant-derived molecules including proteins and amino sugars are degraded through soil profiles and transformed into microbially-derived byproducts that are stabilized via organo-mineral associations;[96-98] whereas more chemically recalcitrant compounds (e.g., lignins and tannin) are preserved due to their lower thermodynamic bioavailability.[99-101] Coincident decreases in SOM diversity from surface to subsoils were also associated with decreases in potential soil respiration (Figure 3b-c), further supporting a link between SOM pool composition and microbial decomposition.[101, 102] The comparatively diverse SOM pools in surface soils contained more bioavailable compounds than subsoils, including protein-, amino sugar-, and lipid-like compounds.[103, 104] The number of formulae in these chemical classes declined with depth, and formula that were common to both soil layers primarily included chemical classes with low putative bioavailability such as lignin-, tannin-, and condensed hydrocarbon-like compounds.[104]

Given that not all chemical constituents of SOM contribute to soil respiration and that surface and subsoils differ substantially in mineralogy and structure, we hypothesized that distinct subsets of SOM would contribute to respiration in surface vs. subsoils. There was no single NMF that dominated low- vs. high-potential respiration soils in either layer, however, NMF weightings varied substantially across soils with different rates of potential respiration in both layers (Figure 4d-e). This suggests that different subsets of SOM were disproportionately associated with soils exhibiting high vs. low potential respiration rates. While patterns in SOM chemical across

geographic regions were difficult to disentangle, the spatial distribution of NMF types suggested local similarity in SOM composition in both layers (Figure S6-7), likely reflecting similar underlying chemistry, mineralogy, and/or biogeochemical processes.[95]

The SOM formula within NMFs that correspond to changes in soil respiration may represent a key step forward in understanding the chemical bioavailability of water-extractable organic matter in soils. In surface soils, NMF6 displayed a dramatic increase in weightings from low-to-high respiration soils. It contained a diverse suite of compounds including protein-, (soluble) lipid-, and amino sugar-like formula that can be rapidly used as microbial substrate. Proteins and amino sugars can fuel microbial metabolism of SOM,[105, 106] thus the prevalence of these compounds within NMF6 may support high potential rates of soil respiration. NMF1 and NMF7 in surface soils contained a diverse mixture of compounds and also increased from low-to-high respiration soils, supporting a possible relationship between SOM pool diversity and microbial respiration (see previous section). In contrast, surface NMF2, NMF3 and NMF5 decreased in importance from low-to-high respiration soils and primarily consisted of a small but unique subset of lignin- and tannin-like compounds (Figure 4a). This is consistent with low bioavailability of its chemical constituents suppressing microbial respiration.[100, 104] It suggests that despite the often-inferred high bioavailability of water-extractable SOM,[41, 107] there may be a significant fraction of water-extractable SOM that is chemically protected from microbial decomposition.[40, 41, 106] Interestingly, NMF4 in surface soils — which contained the greatest number of lipid-like formula (Figure 4a) and had a comparatively large fraction of protein-like formula —was not present in any high-respiration soils. We therefore suggest that NMF4 may be an indicator of non-living microbial biomass (i.e., necromass) which is disproportionately comprised of lipids (microbial cell wall remnants) and amino sugars and proteins (the basis of intracellular materials) [108, 109]. Alternatively, the large number of lipid-like compounds in NMF4 could represent plant-derived lipids that are thought to be resistant to decomposition.[110]

The comparatively weak relationship between subsoil water-extractable SOM and potential soil respiration as compared to surface soils highlights recent work emphasizing the importance of mineral-associated organic matter in soil C storage.[111-113] In subsoils, NMF4 (associated with high-respiration soils) and NMF5 (associated with low-respiration soils) had the largest

disparities in weighting across subsoils (Figure 4e). Consistent with observations from surface soils, subsoil NMF4 contained the largest proportion of amino sugar- and protein-like formula compared to other subsoil NMFs, while NMF5 was almost entirely composed of lignin- and tannin-like compounds.[104] The composition of water-extractable SOM in mineral subsoils is an emerging area of research, and it remains unclear how different SOM chemistries contribute to subsoil respiration.[99] Our results suggest some consistencies in the chemical mechanisms of SOM bioavailability across soil horizons. However, one subsoil NMF (NMF2) had unexpectedly large weightings in high respiration subsoils despite low bioavailability typically associated with its chemical constituents.[104, 114] The remaining subsoil NMFs (1 and 3) were present in both low- and high-respiration subsoils. This denotes that factors beyond chemical recalcitrance or beyond the most commonly measured (water-extractable) SOM pool are critical to understanding belowground C cycling.[109, 115]

Relative importance of physicochemistry and SOM composition in predicting potential soil respiration

By developing machine learning models to predict respiration with soil physicochemistry and SOM composition (NMFs) separately and in combination, we were able to distinguish the contributions of each set of factors for predicting soil potential respiration. The models based on physicochemistry alone explained a modest amount of variation in soil respiration (44% and 43% in surface and subsoils, respectively), in line with the range of explanatory power observed in other works.[116, 117] The most important predictors identified by the physiocochemical models (total C, total N, and CEC for surface soils, CEC for subsoils) were consistent with the variables with the highest independent correlations to potential soil respiration (Table S1).

For surface soils, models based on SOM composition alone (54% variation explained) and both physiocochemical factors and SOM composition combined (62% variation explained) suggest that SOM composition (1) can predict soil respiration at least as well as commonly measured physiocochemical variables and (2) explains some portion of soil respiration that is not captured by physiocochemistry. In models based on SOM composition alone, NMF3 (which was mainly in low-respiration soil and was comprised of lignin- and tannin-like formula, see previous

sections) was the strongest predictor of soil respiration followed by NMF2 and NMF5. The relative chemical recalcitrance of the most important predictors of respiration may suggest that the proportion of thermodynamically unfavorable formula in water-extractable SOM has a direct inhibitory effect on soil metabolism. Indeed, thermodynamic regulation of organic C composition can be a key control for the rate of respiration in ecosystems.[40, 41] Therefore, the inclusion of SOM composition in more mechanistic modeling approaches may be able to improve predictions of soil respiration rates.

However, models for subsoils displayed different dynamics. In the subsoil model based on physicochemical variables alone, total C was the least important predictor (vs. the most important predictor for surface soils), and the model containing SOM composition did not yield high predictive power. We also observed a similar pattern in the partial dependence of soil potential respiration to soil total C across the layers (Figure S10). The marginal effect of total C to surface soil respiration was stronger than the effect on subsoil respiration, supporting a stronger association between total C and potential respiration in surface soil vs. subsoil. The low predictive power of total C relative to other physicochemical factors could explain why SOM composition did not add predictive power to potential respiration in subsoils. Since more total and organic C is stored in surface soils, resolution into the water-extractable SOM pool (reflected here by NMFs) might be a more significant factor for predicting surface soil respiration than in subsoils that are characterized by lower total C and more mineral-associated SOM.[99]

Our results suggest that NMF-extracted signatures of SOM composition are able to improve surface soil model performance by integrating fundamental molecular information into soil respiration models across very different soil ecosystems at the continental scale. NMF6, which was the most important NMF signature in combined models of surface respiration, consisted of diverse chemically-bioavailable compounds, and it mainly existed in high-respiration soils (see previous sections).[104] We therefore suggest that chemically-bioavailable compounds in water-extractable SOM pools may provide the greatest complementary explanatory power to physicochemical factors in respiration predictions. Because SOM pools vary tremendously at the continental-scale, refined regional or local studies that encompass lower-variability parameter spaces may yield even more value of SOM molecular data to soil C modeling.

We note that physicochemical predictors were stronger predictors of soil respiration than SOM composition in the combined surface soil models. However, the inclusion of SOM composition improved physicochemistry-only models by 18%, indicating that it may significantly impact our ability to predict the rate of soil C cycling processes. Future modeling with carefully applied machine learning approaches may open up new avenues for further extracting the relevant portions of SOM pools for inclusion in climate models.

Conclusion

Leveraging molecular information of SOM chemistry to improve conceptualizations and models of soil C cycling is a pressing challenge for global biogeochemical and climate predictions. In this study, we use machine learning (NMF*k*) to distill the thousands of SOM molecules detected by ultrahigh resolution mass spectrometry in soil cores across the continental United States into tractable units. We disentangle these signatures of SOM composition into compounds that are associated with soils exhibiting low versus high rates of potential respiration. These compounds are consistent with prevailing understandings of SOM bioavailability and further suggest chemical recalcitrance as an important mechanism of soil C stabilization in surface soils. Additionally, SOM chemistry (as summarized by NMF*k*) explained a greater proportion of potential soil respiration than commonly measured physicochemical factors, and provided additional explanatory power beyond these factors in combined models. Our results provide a basis for molecular information to spur the development of new process-based representations of soil C cycles and underscore the role of specific chemical constituents within the water-extractable SOM as a determinant of soil respiration.

Acknowledgement

Soil data were provided by the Molecular Observation Network (MONet) at the Environmental Molecular Sciences Laboratory (https://ror.org/04rc0xn13), a DOE Office of Science user facility sponsored by the Biological and Environmental Research program under Contract No. DE-AC05-76RL01830. The work (proposal: 10.46936/10.25585/60008970) conducted by the U.S. Department of Energy, Joint Genome Institute (https://ror.org/04xm1d337), a DOE Office

of Science user facility, is supported by the Office of Science of the U.S. Department of Energy operated under Contract No. DE-AC02-05CH11231.

The Molecular Observation Network (MONet) database is an open, FAIR, and publicly available compilation of the molecular and microstructural properties of soil. Data in the MONet open science database can be found at https://www.emsl.pnnl.gov/monet.

References

1. Giardina, C. P.; Litton, C. M.; Crow, S. E.; Asner, G. P., Warming-related increases in soil CO2 efflux are explained by increased below-ground carbon flux. *Nature Climate Change* **2014,** *4*, (9), 822-827.
2. Jian, J.; Vargas, R.; Anderson-Teixeira, K.; Stell, E.; Herrmann, V.; Horn, M.; Kholod, N.; Manzon, J.; Marchesi, R.; Paredes, D.; Bond-Lamberty, B., A restructured and updated global soil respiration database (SRDB-V5). *Earth Syst. Sci. Data* **2021,** *13*, (2), 255-267.
3. Friedlingstein, P.; O'Sullivan, M.; Jones, M. W.; Andrew, R. M.; Gregor, L.; Hauck, J.; Le Quéré, C.; Luijkx, I. T.; Olsen, A.; Peters, G. P.; Peters, W.; Pongratz, J.; Schwingshackl, C.; Sitch, S.; Canadell, J. G.; Ciais, P.; Jackson, R. B.; Alin, S. R.; Alkama, R.; Arneth, A.; Arora, V. K.; Bates, N. R.; Becker, M.; Bellouin, N.; Bittig, H. C.; Bopp, L.; Chevallier, F.; Chini, L. P.; Cronin, M.; Evans, W.; Falk, S.; Feely, R. A.; Gasser, T.; Gehlen, M.; Gkritzalis, T.; Gloege, L.; Grassi, G.; Gruber, N.; Gürses, Ö.; Harris, I.; Hefner, M.; Houghton, R. A.; Hurtt, G. C.; Iida, Y.; Ilyina, T.; Jain, A. K.; Jersild, A.; Kadono, K.; Kato, E.; Kennedy, D.; Klein Goldewijk, K.; Knauer, J.; Korsbakken, J. I.; Landschützer, P.; Lefèvre, N.; Lindsay, K.; Liu, J.; Liu, Z.; Marland, G.; Mayot, N.; McGrath, M. J.; Metzl, N.; Monacci, N. M.; Munro, D. R.; Nakaoka, S. I.; Niwa, Y.; O'Brien, K.; Ono, T.; Palmer, P. I.; Pan, N.; Pierrot, D.; Pocock, K.; Poulter, B.; Resplandy, L.; Robertson, E.; Rödenbeck, C.; Rodriguez, C.; Rosan, T. M.; Schwinger, J.; Séférian, R.; Shutler, J. D.; Skjelvan, I.; Steinhoff, T.; Sun, Q.; Sutton, A. J.; Sweeney, C.; Takao, S.; Tanhua, T.; Tans, P. P.; Tian, X.; Tian, H.; Tilbrook, B.; Tsujino, H.; Tubiello, F.; van der Werf, G. R.; Walker, A. P.; Wanninkhof, R.; Whitehead, C.; Willstrand Wranne, A.; Wright, R.; Yuan, W.; Yue, C.; Yue, X.; Zaehle, S.; Zeng, J.; Zheng, B., Global Carbon Budget 2022. *Earth Syst. Sci. Data* **2022,** *14*, (11), 4811-4900.
4. Graham, E. B.; Hofmockel, K. S., Ecological stoichiometry as a foundation for omics-enabled biogeochemical models of soil organic matter decomposition. *Biogeochemistry* **2022,** *157*, (1), 31-50.
5. Lei, J.; Guo, X.; Zeng, Y.; Zhou, J.; Gao, Q.; Yang, Y., Temporal changes in global soil respiration since 1987. *Nature communications* **2021,** *12*, (1), 403.
6. Nissan, A.; Alcolombri, U.; Peleg, N.; Galili, N.; Jimenez-Martinez, J.; Molnar, P.; Holzner, M., Global warming accelerates soil heterotrophic respiration. *Nature Communications* **2023,** *14*, (1), 3452.
7. Melillo, J. M.; Frey, S. D.; DeAngelis, K. M.; Werner, W. J.; Bernard, M. J.; Bowles, F. P.; Pold, G.; Knorr, M. A.; Grandy, A. S., Long-term pattern and magnitude of soil carbon feedback to the climate system in a warming world. *Science* **2017,** *358*, (6359), 101-105.
8. Bond-Lamberty, B.; Thomson, A., Temperature-associated increases in the global soil respiration record. *Nature* **2010,** *464*, (7288), 579-582.
9. Todd-Brown, K. E.; Randerson, J. T.; Post, W. M.; Hoffman, F. M.; Tarnocai, C.; Schuur, E. A.; Allison, S. D., Causes of variation in soil carbon simulations from CMIP5 Earth system models and comparison with observations. *Biogeosciences* **2013,** *10*, (3), 1717-1736.
10. Todd-Brown, K.; Randerson, J.; Hopkins, F.; Arora, V.; Hajima, T.; Jones, C.; Shevliakova, E.; Tjiputra, J.; Volodin, E.; Wu, T., Changes in soil organic carbon storage predicted by Earth system models during the 21st century. *Biogeosciences* **2014,** *11*, (8), 2341-2356.
11. Bradford, M. A.; Wieder, W. R.; Bonan, G. B.; Fierer, N.; Raymond, P. A.; Crowther, T. W., Managing uncertainty in soil carbon feedbacks to climate change. *Nature Climate Change* **2016,** *6*, (8), 751-758.
12. Davidson, E. A.; Janssens, I. A., Temperature sensitivity of soil carbon decomposition and feedbacks to climate change. *Nature* **2006,** *440*, (7081), 165-173.
13. Warner, D.; Bond-Lamberty, B.; Jian, J.; Stell, E.; Vargas, R., Spatial predictions and associated uncertainty of annual soil respiration at the global scale. *Global Biogeochemical Cycles* **2019,** *33*, (12), 1733-1745.
14. Crowther, T. W.; Todd-Brown, K. E. O.; Rowe, C. W.; Wieder, W. R.; Carey, J. C.; Machmuller, M. B.; Snoek, B. L.; Fang, S.; Zhou, G.; Allison, S. D.; Blair, J. M.; Bridgham, S. D.; Burton, A. J.; Carrillo, Y.; Reich, P. B.; Clark, J. S.; Classen, A. T.; Dijkstra, F. A.; Elberling, B.; Emmett, B. A.; Estiarte, M.; Frey, S. D.; Guo, J.; Harte, J.; Jiang, L.; Johnson, B. R.; Kröel-Dulay, G.; Larsen, K. S.; Laudon, H.; Lavallee, J. M.; Luo, Y.; Lupascu, M.; Ma, L. N.; Marhan, S.; Michelsen, A.; Mohan, J.; Niu, S.; Pendall, E.; Peñuelas, J.; Pfeifer-Meister, L.; Poll, C.; Reinsch, S.; Reynolds, L. L.; Schmidt, I. K.; Sistla, S.; Sokol, N. W.; Templer, P. H.; Treseder, K. K.; Welker, J. M.; Bradford, M. A., Quantifying global soil carbon losses in response to warming. *Nature* **2016,** *540*, (7631), 104-108.
15. Billings, S. A.; Lajtha, K.; Malhotra, A.; Berhe, A. A.; de Graaff, M. A.; Earl, S.; Fraterrigo, J.; Georgiou, K.; Grandy, S.; Hobbie, S. E., Soil organic carbon is not just for soil scientists: measurement recommendations for diverse practitioners. *Ecological Applications* **2021,** *31*, (3), e02290.

16. Liang, C.; Amelung, W.; Lehmann, J.; Kästner, M., Quantitative assessment of microbial necromass contribution to soil organic matter. *Global change biology* **2019,** *25*, (11), 3578-3590.
17. Sanderman, J.; Baldock, J. A.; Dangal, S. R. S.; Ludwig, S.; Potter, S.; Rivard, C.; Savage, K., Soil organic carbon fractions in the Great Plains of the United States: an application of mid-infrared spectroscopy. *Biogeochemistry* **2021,** *156*, (1), 97-114.
18. Bahureksa, W.; Tfaily, M. M.; Boiteau, R. M.; Young, R. B.; Logan, M. N.; McKenna, A. M.; Borch, T., Soil organic matter characterization by Fourier transform ion cyclotron resonance mass spectrometry (FTICR MS): A critical review of sample preparation, analysis, and data interpretation. *Environmental science & technology* **2021,** *55*, (14), 9637-9656.
19. Cotrufo, M. F.; Wallenstein, M. D.; Boot, C. M.; Denef, K.; Paul, E., The M icrobial E fficiency-M atrix S tabilization (MEMS) framework integrates plant litter decomposition with soil organic matter stabilization: Do labile plant inputs form stable soil organic matter? *Global change biology* **2013,** *19*, (4), 988-995.
20. Sulman, B. N.; Phillips, R. P.; Oishi, A. C.; Shevliakova, E.; Pacala, S. W., Microbe-driven turnover offsets mineral-mediated storage of soil carbon under elevated CO2. *Nature Climate Change* **2014,** *4*, (12), 1099-1102.
21. Robertson, A. D.; Paustian, K.; Ogle, S.; Wallenstein, M. D.; Lugato, E.; Cotrufo, M. F., Unifying soil organic matter formation and persistence frameworks: the MEMS model. *Biogeosciences* **2019,** *16*, (6), 1225-1248.
22. Falloon, P.; Jones, C. D.; Ades, M.; Paul, K., Direct soil moisture controls of future global soil carbon changes: An important source of uncertainty. *Global Biogeochemical Cycles* **2011,** *25*, (3).
23. Ciais, P.; Sabine, C.; Bala, G.; Bopp, L.; Brovkin, V.; Canadell, J.; Chhabra, A.; DeFries, R.; Galloway, J.; Heimann, M., Carbon and other biogeochemical cycles. In *Climate change 2013: the physical science basis. Contribution of Working Group I to the Fifth Assessment Report of the Intergovernmental Panel on Climate Change*, Cambridge University Press: 2014; pp 465-570.
24. Amador, J.; Jones, R. D., Nutrient limitations on microbial respiration in peat soils with different total phosphorus content. *Soil Biology and Biochemistry* **1993,** *25*, (6), 793-801.
25. Malik, A. A.; Puissant, J.; Buckeridge, K. M.; Goodall, T.; Jehmlich, N.; Chowdhury, S.; Gweon, H. S.; Peyton, J. M.; Mason, K. E.; van Agtmaal, M., Land use driven change in soil pH affects microbial carbon cycling processes. *Nature communications* **2018,** *9*, (1), 3591.
26. Fang, C.; Moncrieff, J. B., The variation of soil microbial respiration with depth in relation to soil carbon composition. *Plant and Soil* **2005,** *268*, 243-253.
27. Curiel Yuste, J.; Baldocchi, D.; Gershenson, A.; Goldstein, A.; Misson, L.; Wong, S., Microbial soil respiration and its dependency on carbon inputs, soil temperature and moisture. *Global Change Biology* **2007,** *13*, (9), 2018-2035.
28. Billings, S. A.; Ballantyne IV, F., How interactions between microbial resource demands, soil organic matter stoichiometry, and substrate reactivity determine the direction and magnitude of soil respiratory responses to warming. *Global Change Biology* **2013,** *19*, (1), 90-102.
29. Raich, J. W.; Potter, C. S., Global patterns of carbon dioxide emissions from soils. *Global biogeochemical cycles* **1995,** *9*, (1), 23-36.
30. Raich, J. W.; Potter, C. S.; Bhagawati, D., Interannual variability in global soil respiration, 1980–94. *Global Change Biology* **2002,** *8*, (8), 800-812.
31. Kyker-Snowman, E.; Wieder, W. R.; Frey, S. D.; Grandy, A. S., Stoichiometrically coupled carbon and nitrogen cycling in the MIcrobial-MIneral Carbon Stabilization model version 1.0 (MIMICS-CN v1. 0). *Geoscientific Model Development* **2020,** *13*, (9), 4413-4434.
32. Wieder, W. R.; Hartman, M. D.; Sulman, B. N.; Wang, Y. P.; Koven, C. D.; Bonan, G. B., Carbon cycle confidence and uncertainty: Exploring variation among soil biogeochemical models. *Global change biology* **2018,** *24*, (4), 1563-1579.
33. Waring, B. G.; Sulman, B. N.; Reed, S.; Smith, A. P.; Averill, C.; Creamer, C. A.; Cusack, D. F.; Hall, S. J.; Jastrow, J. D.; Jilling, A., From pools to flow: The PROMISE framework for new insights on soil carbon cycling in a changing world. *Global Change Biology* **2020,** *26*, (12), 6631-6643.
34. Song, H.-S.; Stegen, J. C.; Graham, E. B.; Lee, J.-Y.; Garayburu-Caruso, V. A.; Nelson, W. C.; Chen, X.; Moulton, J. D.; Scheibe, T. D., Representing organic matter thermodynamics in biogeochemical reactions via substrate-explicit modeling. *Frontiers in Microbiology* **2020,** *11*, 531756.
35. Bradford, M. A.; Wood, S. A.; Addicott, E. T.; Fenichel, E. P.; Fields, N.; González-Rivero, J.; Jevon, F. V.; Maynard, D. S.; Oldfield, E. E.; Polussa, A.; Ward, E. B.; Wieder, W. R., Quantifying microbial control of soil organic matter dynamics at macrosystem scales. *Biogeochemistry* **2021,** *156*, (1), 19-40.
36. Hall, S. J.; Ye, C.; Weintraub, S. R.; Hockaday, W. C., Molecular trade-offs in soil organic carbon composition at continental scale. *Nature Geoscience* **2020,** *13*, (10), 687-692.

37. Huys, R.; Poirier, V.; Bourget, M. Y.; Roumet, C.; Hättenschwiler, S.; Fromin, N.; Munson, A. D.; Freschet, G. T., Plant litter chemistry controls coarse-textured soil carbon dynamics. *Journal of Ecology* **2022,** *110*, (12), 2911-2928.
38. Scott, N. A.; Cole, C. V.; Elliott, E. T.; Huffman, S. A., Soil textural control on decomposition and soil organic matter dynamics. *Soil Science Society of America Journal* **1996,** *60*, (4), 1102-1109.
39. Witzgall, K.; Vidal, A.; Schubert, D. I.; Höschen, C.; Schweizer, S. A.; Buegger, F.; Pouteau, V.; Chenu, C.; Mueller, C. W., Particulate organic matter as a functional soil component for persistent soil organic carbon. *Nature Communications* **2021,** *12*, (1), 4115.
40. Tureţcaia, A. B.; Garayburu-Caruso, V. A.; Kaufman, M. H.; Danczak, R. E.; Stegen, J. C.; Chu, R. K.; Toyoda, J. G.; Cardenas, M. B.; Graham, E. B., Rethinking Aerobic Respiration in the Hyporheic Zone under Variation in Carbon and Nitrogen Stoichiometry. *Environmental Science & Technology* **2023,** *57*, (41), 15499-15510.
41. Garayburu-Caruso, V. A.; Stegen, J. C.; Song, H.-S.; Renteria, L.; Wells, J.; Garcia, W.; Resch, C. T.; Goldman, A. E.; Chu, R. K.; Toyoda, J., Carbon limitation leads to thermodynamic regulation of aerobic metabolism. *Environmental Science & Technology Letters* **2020,** *7*, (7), 517-524.
42. Hodgkins, S. B.; Tfaily, M. M.; McCalley, C. K.; Logan, T. A.; Crill, P. M.; Saleska, S. R.; Rich, V. I.; Chanton, J. P., Changes in peat chemistry associated with permafrost thaw increase greenhouse gas production. *Proceedings of the National Academy of Sciences* **2014,** *111*, (16), 5819-5824.
43. Li, H.; Bölscher, T.; Winnick, M.; Tfaily, M. M.; Cardon, Z. G.; Keiluweit, M., Simple plant and microbial exudates destabilize mineral-associated organic matter via multiple pathways. *Environmental science & technology* **2021,** *55*, (5), 3389-3398.
44. Graham, E. B.; Crump, A. R.; Kennedy, D. W.; Arntzen, E.; Fansler, S.; Purvine, S. O.; Nicora, C. D.; Nelson, W.; Tfaily, M. M.; Stegen, J. C., Multi'omics comparison reveals metabolome biochemistry, not microbiome composition or gene expression, corresponds to elevated biogeochemical function in the hyporheic zone. *Science of the total environment* **2018,** *642*, 742-753.
45. Graham, E. B.; Tfaily, M. M.; Crump, A. R.; Goldman, A. E.; Bramer, L. M.; Arntzen, E.; Romero, E.; Resch, C. T.; Kennedy, D. W.; Stegen, J. C., Carbon inputs from riparian vegetation limit oxidation of physically bound organic carbon via biochemical and thermodynamic processes. *Journal of Geophysical Research: Biogeosciences* **2017,** *122*, (12), 3188-3205.
46. Sonnewald, M.; Dutkiewicz, S.; Hill, C.; Forget, G., Elucidating ecological complexity: Unsupervised learning determines global marine eco-provinces. *Science Advances* **2020,** *6*, (22), eaay4740.
47. Nishiyama, E.; Higashi, K.; Mori, H.; Suda, K.; Nakamura, H.; Omori, S.; Maruyama, S.; Hongoh, Y.; Kurokawa, K., The Relationship Between Microbial Community Structures and Environmental Parameters Revealed by Metagenomic Analysis of Hot Spring Water in the Kirishima Area, Japan. *Frontiers in bioengineering and biotechnology* **2018,** *6*, 202.
48. Ortner, M.; Seidel, M.; Semella, S.; Udelhoven, T.; Vohland, M.; Thiele-Bruhn, S., Content of soil organic carbon and labile fractions depend on local combinations of mineral-phase characteristics. *SOIL* **2022,** *8*, (1), 113-131.
49. Ukalska-Jaruga, A.; Smreczak, B.; Klimkowicz-Pawlas, A., Soil organic matter composition as a factor affecting the accumulation of polycyclic aromatic hydrocarbons. *Journal of Soils and Sediments* **2019,** *19*, (4), 1890-1900.
50. Shigyo, N.; Furusawa, H.; Yamashita, N.; Nagakura, J.; Manaka, T.; Yamada, T.; Hirai, K., Slope-induced factors shape bacterial communities in surface soils in a forested headwater catchment. *CATENA* **2022,** *214*, 106253.
51. Massoni, J.; Bortfeld-Miller, M.; Widmer, A.; Vorholt, J. A., Capacity of soil bacteria to reach the phyllosphere and convergence of floral communities despite soil microbiota variation. *Proceedings of the National Academy of Sciences* **2021,** *118*, (41), e2100150118.
52. Simister, R. L.; Iulianella Phillips, B. P.; Wickham, A. P.; Cayer, E. M.; Hart, C. J. R.; Winterburn, P. A.; Crowe, S. A., DNA sequencing, microbial indicators, and the discovery of buried kimberlites. *Communications Earth & Environment* **2023,** *4*, (1), 387.
53. Bowman, M. M.; Heath, A. E.; Varga, T.; Battu, A. K.; Chu, R. K.; Toyoda, J.; Cheeke, T. E.; Porter, S. S.; Moffett, K. B.; LeTendre, B.; Qafoku, O.; Bargar, J. R.; Mans, D. M.; Hess, N. J.; Graham, E. B., One thousand soils for molecular understanding of belowground carbon cycling. *Frontiers in Soil Science* **2023,** *3*.
54. Brookes, P.; Landman, A.; Pruden, G.; Jenkinson, D., Chloroform fumigation and the release of soil nitrogen: a rapid direct extraction method to measure microbial biomass nitrogen in soil. *Soil biology and biochemistry* **1985,** *17*, (6), 837-842.

55. Witt, C.; Gaunt, J. L.; Galicia, C. C.; Ottow, J. C.; Neue, H.-U., A rapid chloroform-fumigation extraction method for measuring soil microbial biomass carbon and nitrogen in flooded rice soils. *Biology and Fertility of Soils* **2000,** *30*, 510-519.
56. Zhao, Q.; Thompson, A. M.; Callister, S. J.; Tfaily, M. M.; Bell, S. L.; Hobbie, S. E.; Hofmockel, K. S., Dynamics of organic matter molecular composition under aerobic decomposition and their response to the nitrogen addition in grassland soils. *Science of the Total Environment* **2022,** *806*, 150514.
57. Corbridge, D. E. C., *Phosphorus. An outline of its chemistry, biochemistry, and technology*. Elsevier Scientific Co.: 1980.
58. Bray, R. H.; Kurtz, L. T., Determination of total, organic, and available forms of phosphorus in soils. *Soil science* **1945,** *59*, (1), 39-46.
59. AOAC, I., AOAC Official Method 972.43, Microchemical determination of carbon, hydrogen, and nitrogen, automated method. *Official Methods of Analysis of AOAC International. AOAC International, Gaithersburg, MD* **2006**, 5-6.
60. Dittmar, T.; Koch, B.; Hertkorn, N.; Kattner, G., A simple and efficient method for the solid-phase extraction of dissolved organic matter (SPE-DOM) from seawater. *Limnology and Oceanography: Methods* **2008,** *6*, (6), 230-235.
61. Corilo, Y.; Kew, W.; McCue, L., EMSL-Computing/CoreMS: CoreMS 1.0. 0 (v1. 0.0). *Zenodo10* **2021,** *5281*.
62. Kim, S.; Kramer, R. W.; Hatcher, P. G., Graphical method for analysis of ultrahigh-resolution broadband mass spectra of natural organic matter, the van Krevelen diagram. *Analytical chemistry* **2003,** *75*, (20), 5336-5344.
63. Tfaily, M. M.; Chu, R. K.; Tolić, N.; Roscioli, K. M.; Anderton, C. R.; Paša-Tolić, L.; Robinson, E. W.; Hess, N. J., Advanced solvent based methods for molecular characterization of soil organic matter by high-resolution mass spectrometry. *Analytical chemistry* **2015,** *87*, (10), 5206-5215.
64. Lee, D.; Seung, H. S., Algorithms for non-negative matrix factorization. *Advances in neural information processing systems* **2000,** *13*.
65. Bhattarai, M.; Chennupati, G.; Skau, E.; Vangara, R.; Djidjev, H.; Alexandrov, B. S. In *Distributed Non-Negative Tensor Train Decomposition*, 2020 IEEE High Performance Extreme Computing Conference (HPEC), 22-24 Sept. 2020, 2020; 2020; pp 1-10.
66. Devarajan, K., Nonnegative Matrix Factorization: An Analytical and Interpretive Tool in Computational Biology. *PLOS Computational Biology* **2008,** *4*, (7), e1000029.
67. Bholowalia, P.; Kumar, A., EBK-means: A clustering technique based on elbow method and k-means in WSN. *International Journal of Computer Applications* **2014,** *105*, (9).
68. Riaz, M.; Marschner, P., Sandy Soil Amended with Clay Soil: Effect of Clay Soil Properties on Soil Respiration, Microbial Biomass, and Water Extractable Organic C. *Journal of Soil Science and Plant Nutrition* **2020,** *20*, (4), 2465-2470.
69. Lee, K.-H.; Jose, S., Soil respiration, fine root production, and microbial biomass in cottonwood and loblolly pine plantations along a nitrogen fertilization gradient. *Forest Ecology and Management* **2003,** *185*, (3), 263-273.
70. Chen, S.; Zou, J.; Hu, Z.; Chen, H.; Lu, Y., Global annual soil respiration in relation to climate, soil properties and vegetation characteristics: Summary of available data. *Agricultural and Forest Meteorology* **2014,** *198-199*, 335-346.
71. Orchard, V. A.; Cook, F., Relationship between soil respiration and soil moisture. *Soil Biology and Biochemistry* **1983,** *15*, (4), 447-453.
72. Xu, L.; Baldocchi, D. D.; Tang, J., How soil moisture, rain pulses, and growth alter the response of ecosystem respiration to temperature. *Global Biogeochemical Cycles* **2004,** *18*, (4).
73. Moyano, F. E.; Manzoni, S.; Chenu, C., Responses of soil heterotrophic respiration to moisture availability: An exploration of processes and models. *Soil Biology and Biochemistry* **2013,** *59*, 72-85.
74. Wang, Y.-P.; Houlton, B. Z., Nitrogen constraints on terrestrial carbon uptake: Implications for the global carbon-climate feedback. *Geophysical Research Letters* **2009,** *36*, (24).
75. Elser, J.; Sterner, R.; Gorokhova, E. a.; Fagan, W.; Markow, T.; Cotner, J.; Harrison, J.; Hobbie, S.; Odell, G.; Weider, L., Biological stoichiometry from genes to ecosystems. *Ecology letters* **2000,** *3*, (6), 540-550.
76. Soong, J. L.; Fuchslueger, L.; Marañon-Jimenez, S.; Torn, M. S.; Janssens, I. A.; Penuelas, J.; Richter, A., Microbial carbon limitation: The need for integrating microorganisms into our understanding of ecosystem carbon cycling. *Global change biology* **2020,** *26*, (4), 1953-1961.
77. Fang, C.; Moncrieff, J. B., The variation of soil microbial respiration with depth in relation to soil carbon composition. *Plant and Soil* **2005,** *268*, (1), 243-253.

78. Schimel, J., The Democracy of dirt: relating micro-scale dynamics to macro-scale ecosystem function. *Microbes: The foundation stone of the biosphere* **2021**, 89-102.
79. Nicolás, C.; Martin-Bertelsen, T.; Floudas, D.; Bentzer, J.; Smits, M.; Johansson, T.; Troein, C.; Persson, P.; Tunlid, A., The soil organic matter decomposition mechanisms in ectomycorrhizal fungi are tuned for liberating soil organic nitrogen. *The ISME Journal* **2019,** *13*, (4), 977-988.
80. Subedi, P.; Jokela, E. J.; Vogel, J. G.; Bracho, R.; Inglett, K. S., The effects of nutrient limitations on microbial respiration and organic matter decomposition in a Florida Spodosol as influenced by historical forest management practices. *Forest Ecology and Management* **2021,** *479*, 118592.
81. Mori, T.; Lu, X.; Aoyagi, R.; Mo, J., Reconsidering the phosphorus limitation of soil microbial activity in tropical forests. *Functional Ecology* **2018,** *32*, (5), 1145-1154.
82. Fan, B.; Yin, L.; Dijkstra, F. A.; Lu, J.; Shao, S.; Wang, P.; Wang, Q.; Cheng, W., Potential gross nitrogen mineralization and its linkage with microbial respiration along a forest transect in eastern China. *Applied Soil Ecology* **2022,** *171*, 104347.
83. Gransee, A.; Führs, H., Magnesium mobility in soils as a challenge for soil and plant analysis, magnesium fertilization and root uptake under adverse growth conditions. *Plant and Soil* **2013,** *368*, (1), 5-21.
84. Opfergelt, S.; Cornélis, J. T.; Houben, D.; Givron, C.; Burton, K. W.; Mattielli, N., The influence of weathering and soil organic matter on Zn isotopes in soils. *Chemical Geology* **2017,** *466*, 140-148.
85. Chao, L.; Liu, Y.; Freschet, G. T.; Zhang, W.; Yu, X.; Zheng, W.; Guan, X.; Yang, Q.; Chen, L.; Dijkstra, F. A., Litter carbon and nutrient chemistry control the magnitude of soil priming effect. *Functional Ecology* **2019,** *33*, (5), 876-888.
86. Neupane, A.; Herndon, E. M.; Whitman, T.; Faiia, A. M.; Jagadamma, S., Manganese effects on plant residue decomposition and carbon distribution in soil fractions depend on soil nitrogen availability. *Soil Biology and Biochemistry* **2023,** *178*, 108964.
87. Kranabetter, J. M.; Philpott, T.; Dunn, D., Manganese limitations and the enhanced soil carbon sequestration of temperate rainforests. *Biogeochemistry* **2021,** *156*, (2), 195-209.
88. Santos, F.; Herndon, E., Plant-Soil Relationships Influence Observed Trends Between Manganese and Carbon Across Biomes. *Global Biogeochemical Cycles* **2023,** *37*, (1), e2022GB007412.
89. Li, H.; Santos, F.; Butler, K.; Herndon, E., A critical review on the multiple roles of manganese in stabilizing and destabilizing soil organic matter. *Environmental science & technology* **2021,** *55*, (18), 12136-12152.
90. Whalen, E. D. Manganese Limitation as a Mechanism for Reduced Decomposition in Soils under Long-Term Atmospheric Nitrogen Deposition. University of New Hampshire, 2017.
91. Taylor, P. G.; Townsend, A. R., Stoichiometric control of organic carbon–nitrate relationships from soils to the sea. *Nature* **2010,** *464*, (7292), 1178-1181.
92. Zhang, M.; Zhang, X.; Zhang, L.; Zeng, L.; Liu, Y.; Wang, X.; He, P.; Li, S.; Liang, G.; Zhou, W.; Ai, C., The stronger impact of inorganic nitrogen fertilization on soil bacterial community than organic fertilization in short-term condition. *Geoderma* **2021,** *382*, 114752.
93. Siles, J. A.; Cajthaml, T.; Filipová, A.; Minerbi, S.; Margesin, R., Altitudinal, seasonal and interannual shifts in microbial communities and chemical composition of soil organic matter in Alpine forest soils. *Soil Biology and Biochemistry* **2017,** *112*, 1-13.
94. Berryman, E. M.; Marshall, J. D.; Kavanagh, K., Decoupling litter respiration from whole-soil respiration along an elevation gradient in a Rocky Mountain mixed-conifer forest. *Canadian Journal of Forest Research* **2014,** *44*, (5), 432-440.
95. Brye, K. R.; McMullen, R. L.; Silveira, M. L.; Motschenbacher, J. M. D.; Smith, S. F.; Gbur, E. E.; Helton, M. L., Environmental controls on soil respiration across a southern US climate gradient: a meta-analysis. *Geoderma Regional* **2016,** *7*, (2), 110-119.
96. Kallenbach, C. M.; Frey, S. D.; Grandy, A. S., Direct evidence for microbial-derived soil organic matter formation and its ecophysiological controls. *Nature Communications* **2016,** *7*, (1), 13630.
97. Roth, V.-N.; Lange, M.; Simon, C.; Hertkorn, N.; Bucher, S.; Goodall, T.; Griffiths, R. I.; Mellado-Vázquez, P. G.; Mommer, L.; Oram, N. J.; Weigelt, A.; Dittmar, T.; Gleixner, G., Persistence of dissolved organic matter explained by molecular changes during its passage through soil. *Nature Geoscience* **2019,** *12*, (9), 755-761.
98. Zhao, Q.; Callister, S. J.; Thompson, A. M.; Kukkadapu, R. K.; Tfaily, M. M.; Bramer, L. M.; Qafoku, N. P.; Bell, S. L.; Hobbie, S. E.; Seabloom, E. W.; Borer, E. T.; Hofmockel, K. S., Strong mineralogic control of soil organic matter composition in response to nutrient addition across diverse grassland sites. *Science of The Total Environment* **2020,** *736*, 137839.
99. Rumpel, C.; Kögel-Knabner, I., Deep soil organic matter—a key but poorly understood component of terrestrial C cycle. *Plant and soil* **2011,** *338*, 143-158.

100. Kögel-Knabner, I., The macromolecular organic composition of plant and microbial residues as inputs to soil organic matter. *Soil Biology and Biochemistry* **2002,** *34*, (2), 139-162.
101. Kramer, C.; Gleixner, G., Soil organic matter in soil depth profiles: Distinct carbon preferences of microbial groups during carbon transformation. *Soil Biology and Biochemistry* **2008,** *40*, (2), 425-433.
102. Davenport, R.; Bowen, B. P.; Lynch, L. M.; Kosina, S. M.; Shabtai, I.; Northen, T. R.; Lehmann, J., Decomposition decreases molecular diversity and ecosystem similarity of soil organic matter. *Proceedings of the National Academy of Sciences* **2023,** *120*, (25), e2303335120.
103. Jones, D. L., Amino acid biodegradation and its potential effects on organic nitrogen capture by plants. *Soil biology and biochemistry* **1999,** *31*, (4), 613-622.
104. Marschner, B.; Kalbitz, K., Controls of bioavailability and biodegradability of dissolved organic matter in soils. *Geoderma* **2003,** *113*, (3-4), 211-235.
105. Campbell, T. P.; Ulrich, D. E. M.; Toyoda, J.; Thompson, J.; Munsky, B.; Albright, M. B. N.; Bailey, V. L.; Tfaily, M. M.; Dunbar, J., Microbial Communities Influence Soil Dissolved Organic Carbon Concentration by Altering Metabolite Composition. *Frontiers in Microbiology* **2022,** *12*.
106. Hernández, D. L.; Hobbie, S. E., The effects of substrate composition, quantity, and diversity on microbial activity. *Plant and Soil* **2010,** *335*, (1), 397-411.
107. Marschner, B.; Kalbitz, K., Controls of bioavailability and biodegradability of dissolved organic matter in soils. *Geoderma* **2003,** *113*, (3), 211-235.
108. Camenzind, T.; Mason-Jones, K.; Mansour, I.; Rillig, M. C.; Lehmann, J., Formation of necromass-derived soil organic carbon determined by microbial death pathways. *Nature Geoscience* **2023,** *16*, (2), 115-122.
109. Angst, G.; Mueller, K. E.; Nierop, K. G. J.; Simpson, M. J., Plant- or microbial-derived? A review on the molecular composition of stabilized soil organic matter. *Soil Biology and Biochemistry* **2021,** *156*, 108189.
110. Angst, G.; Mueller, K. E.; Kögel-Knabner, I.; Freeman, K. H.; Mueller, C. W., Aggregation controls the stability of lignin and lipids in clay-sized particulate and mineral associated organic matter. *Biogeochemistry* **2017,** *132*, (3), 307-324.
111. Cotrufo, M. F.; Ranalli, M. G.; Haddix, M. L.; Six, J.; Lugato, E., Soil carbon storage informed by particulate and mineral-associated organic matter. *Nature Geoscience* **2019,** *12*, (12), 989-994.
112. Benbi, D.; Boparai, A.; Brar, K., Decomposition of particulate organic matter is more sensitive to temperature than the mineral associated organic matter. *Soil Biology and Biochemistry* **2014,** *70*, 183-192.
113. Lugato, E.; Lavallee, J. M.; Haddix, M. L.; Panagos, P.; Cotrufo, M. F., Different climate sensitivity of particulate and mineral-associated soil organic matter. *Nature Geoscience* **2021,** *14*, (5), 295-300.
114. Lehmann, J.; Hansel, C. M.; Kaiser, C.; Kleber, M.; Maher, K.; Manzoni, S.; Nunan, N.; Reichstein, M.; Schimel, J. P.; Torn, M. S.; Wieder, W. R.; Kögel-Knabner, I., Persistence of soil organic carbon caused by functional complexity. *Nature Geoscience* **2020,** *13*, (8), 529-534.
115. Zhang, H.; Goll, D. S.; Wang, Y. P.; Ciais, P.; Wieder, W. R.; Abramoff, R.; Huang, Y.; Guenet, B.; Prescher, A. K.; Viscarra Rossel, R. A., Microbial dynamics and soil physicochemical properties explain large-scale variations in soil organic carbon. *Global Change Biology* **2020,** *26*, (4), 2668-2685.
116. Graham, E. B.; Wieder, W. R.; Leff, J. W.; Weintraub, S. R.; Townsend, A. R.; Cleveland, C. C.; Philippot, L.; Nemergut, D. R., Do we need to understand microbial communities to predict ecosystem function? A comparison of statistical models of nitrogen cycling processes. *Soil Biology and Biochemistry* **2014,** *68*, 279-282.
117. Allison, S., A trait-based approach for modelling microbial litter decomposition. *Ecology letters* **2012,** *15*, (9), 1058-1070.

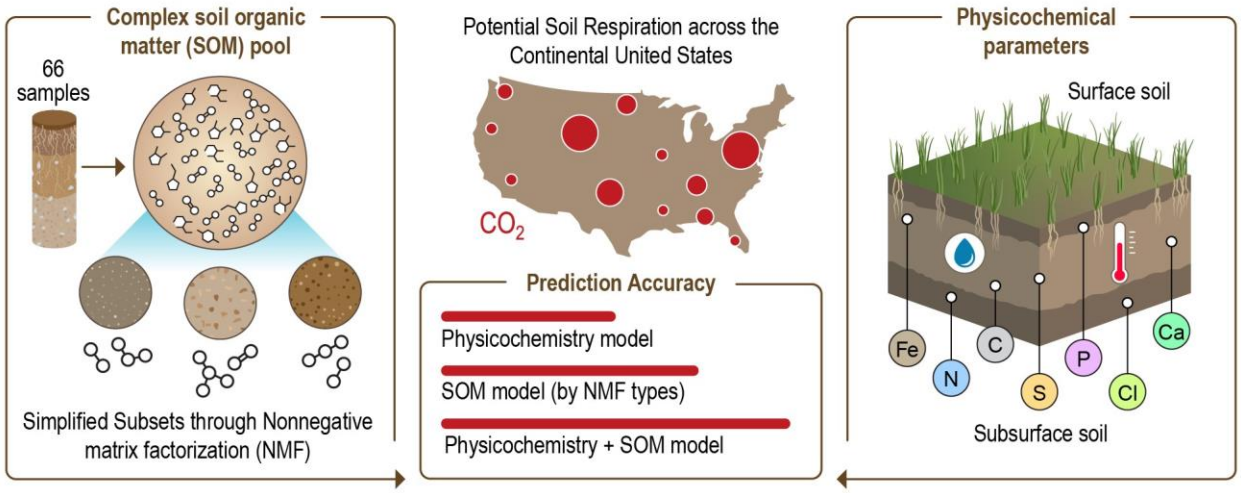

Figure 1. Proposed workflow: Machine learning models summarize molecular data to predict soil respiration. Non-negative matrix factorization (NMF*k*) extracts key SOM signatures from high resolution mass spectrometry measurements of SOM. Gradient boosting regression predicts soil respiration with physicochemistry, SOM signatures, and physicochemistry combined with SOM signatures.

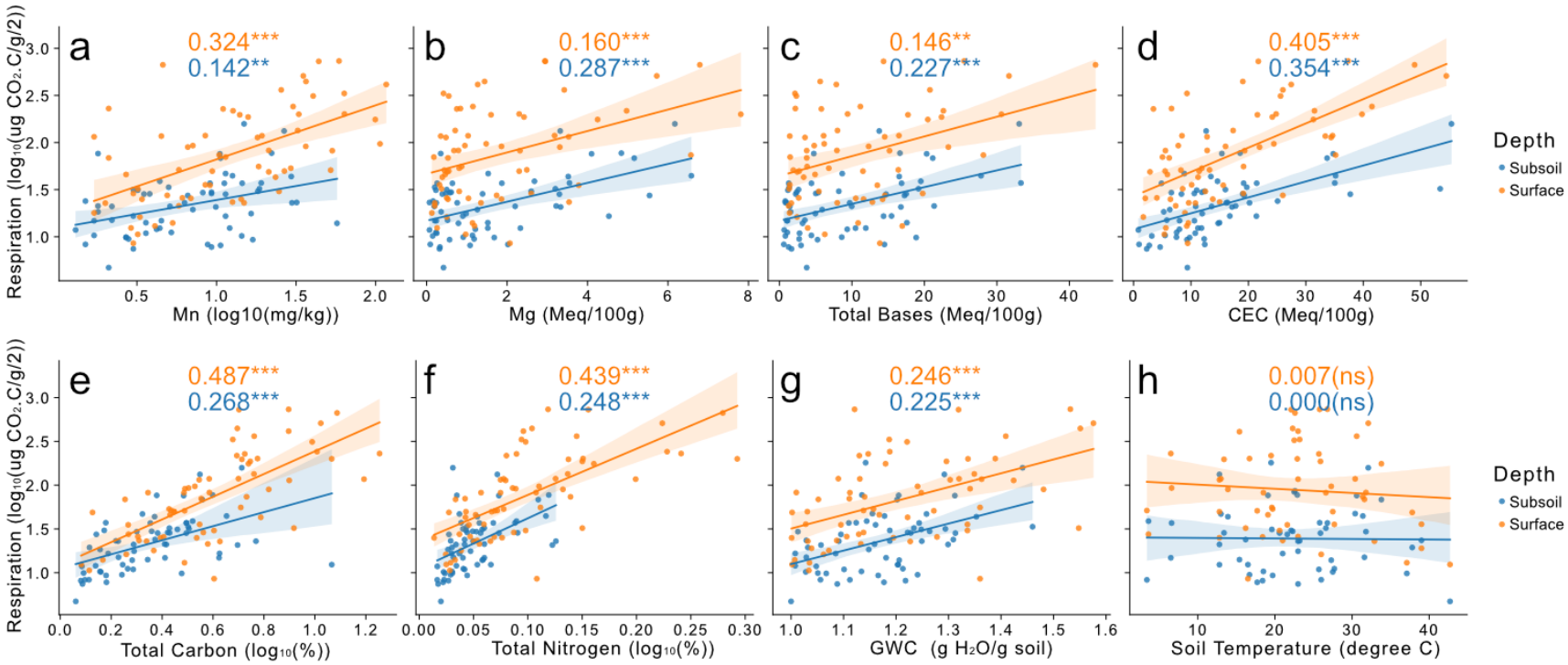

Figure 2. The relationship between soil characteristics and potential respiration. (a-h) show [Manganese(Mn), Magnesium(Mg), Total Bases, CEC, Total C, Total N, GWC, Soil Temperature], respectively. Orange represents surface soils and blue represents subsoils. Lines denote the fitted linear regression function. Numbers on each panel are r^2 value from linear regression, the stars behind represents statistical significance (*** ($p \leq 0.001$), **($p \leq 0.01$), ns ($p > 0.05$)).

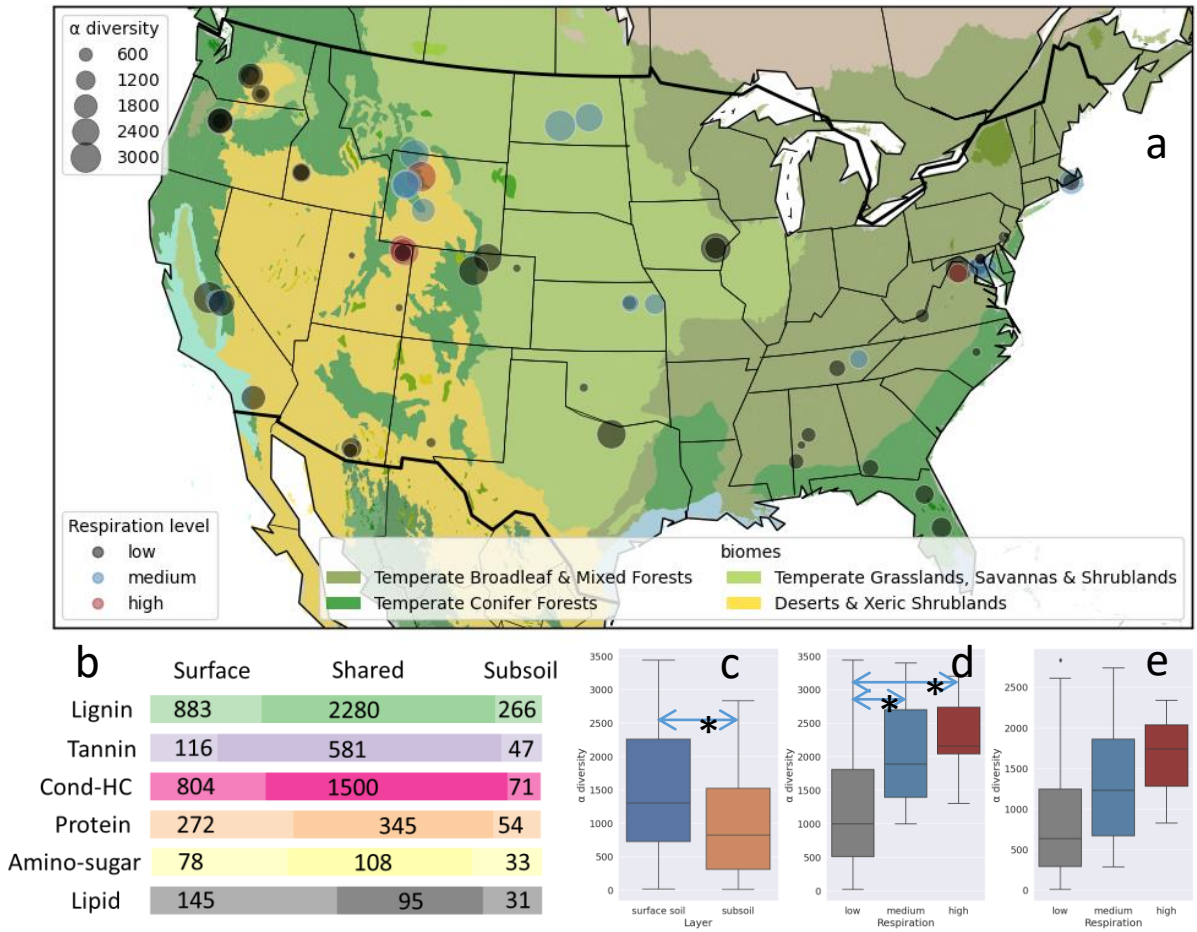

Figure 3. (a) Spatial distribution of soil respiration levels (labeled by colors) and alpha diversity of each sample (sizes). Soil respiration levels are determined by *k*-means clustering on soil respiration rates (ug CO2/g soil/day). Soils from temperate conifer forests and temperate grasslands, savannas & shrublands have relatively higher respiration rates compared to other biomes (Figure S1). (b) The number of shared and unique SOM compound classes identified between surface and subsoils. The classes were suggested by van-Krevelen plot. (c) The difference of alpha diversity in surface and subsoil soils ($p < 0.05$ from ANOVA, *: $p<0.05$ from Tukey's HSD test) (d) the difference of alpha diversity in surface soils with different levels of potential respiration ($p < 0.05$ from ANOVA, *: $p<0.05$ from Tukey's HSD test) (e) the difference of alpha diversity in subsoils with different levels of potential respiration ($p < 0.05$ from ANOVA).

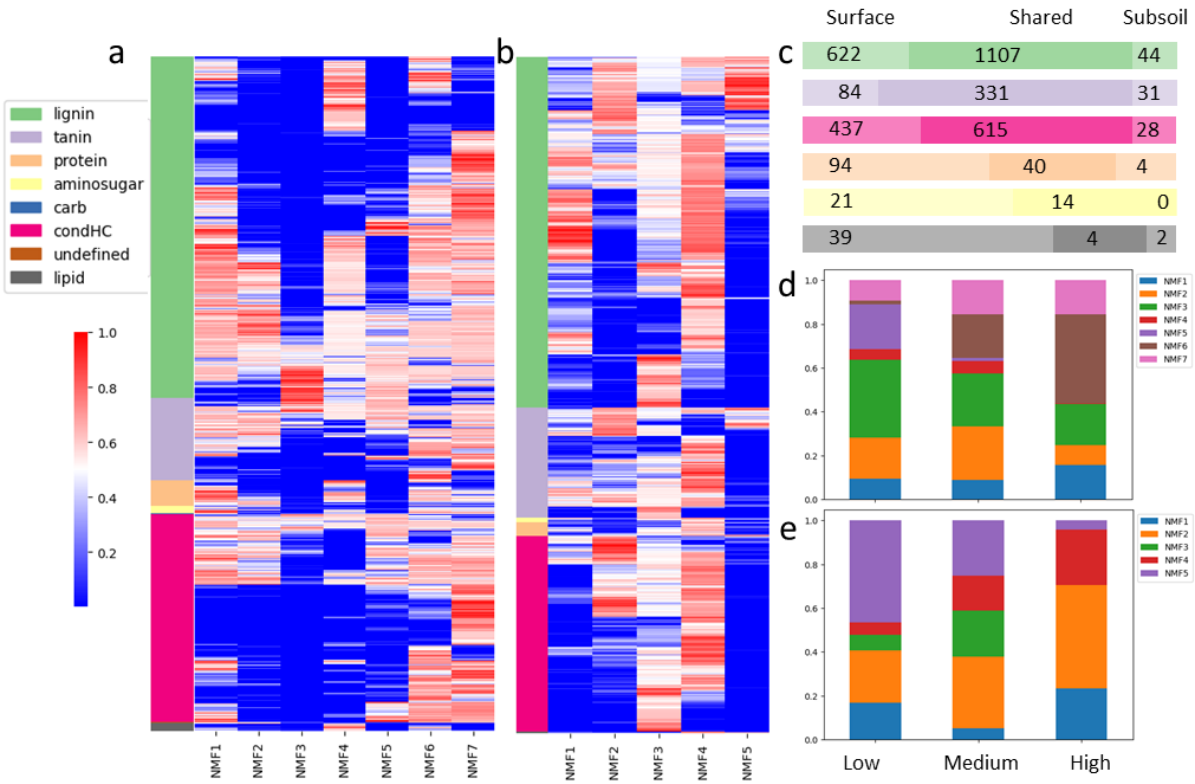

Figure 4. NMF*k* partitioning of SOM composition. (a-b) Relative contribution of organic formula to each SOM signatures identified by NMF*k* in a) surface and b) subsoils. The color in each cell represents the normalized (0 to 1) relative contribution for each SOM feature (row) to each NMF*k* signature (column), red indicates the most important contributor, and blue indicates the least. The side bar indicates the compound class of each SOM feature. (c) The number of shared and unique formula identified as important (normalized weights >0.5) by NMF*k* in surface and subsoils. (d-e) The relative contribution of NMF*k* signatures to each level of respiration rates in both d) surface and e) subsoils. Surface soils: low respiration level (N = 44), medium respiration level (N = 14), high respiration level (N = 5, UT12, UT23, UT24, WY03, Temperate Conifer Forests, SCBI Temperate Broadleaf & Mixed Forests). Subsoils: low respiration level (N = 48), medium respiration level (N =10), high respiration level (N = 3, T12, UT19, Temperate Conifer Forests, WLLO, Temperate Broadleaf & Mixed Forests).

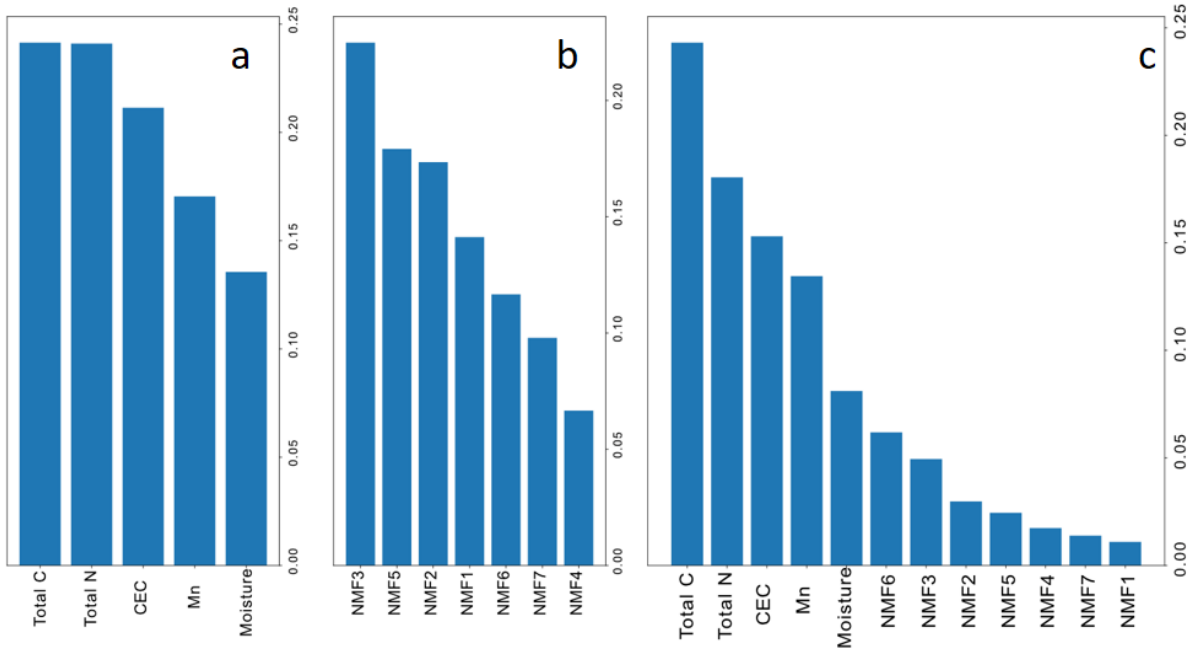

Figure 5. Relative importance of each predictor in surface soil potential respiration machine learning models. a) Physicochemistry model, with physicochemical variables only. b) SOM model, with SOM signatures represented by NMFs only. c) Physicochemistry & SOM model with both physicochemical variables and SOM signatures.

Table 1. Model performance for predictions of potential soil respiration with physicochemical variables (Physiochemistry model), SOM by NMF*k* signatures (SOM_model), and combined physicochemical variables and SOM variables (Physiochemistry &SOM_model) for average 5-fold cross-validation accuracies (training soils, RMSE), and testing sample accuracies (RMSE, R2).

	Physiochemistry Model	SOM_model	Physicochemistry &SOM_model
Surface_CV	0.80	1.05	0.82
Surface_test	0.98	0.89	0.82
Surface_test (R2)	0.44	0.54	0.62
Subsoil_CV	0.60	0.82	0.67
Subsoil_test	0.46	0.80	0.49
Subsoil_test (R2)	0.43	0.08	0.36

Supporting Information of
Soil Organic Matter Composition Improves Predictions of Potential Soil Respiration across the Continental United States

Cheng Shi[a], Maruti Mudunuru[b], Maggie Bowman[c], Qian Zhao[c], Jason Toyoda[c], Will Kew[c], Yuri Corilo[c], Odeta Qafoku[c], John R. Bargar[c], Satish Karra[c], & Emily Graham[d,e*]

[a]Oregon State University, Department of Biological & Ecological Engineering, Corvallis, OR, United States.
[b]Energy and Environment Directorate, Pacific Northwest National Laboratory, Richland, WA, United States.
[c] Environmental Molecular Science Laboratory, Pacific Northwest National Laboratory, Richland, WA, United States.
[d]Earth and Biological Sciences Directorate, *Pacific Northwest National Laboratory, Richland, WA, United States.*
[e]*School of Biological Sciences, Washington State University, Pullman, WA, United States.*

**Corresponding author: emily.graham@pnnl.gov*

NMFk model assumption and robustness

NMF*k* model was selected to decompose the SOM composition matrix into multiple basis signatures, due to its ability to capture unique and sparse characteristics or data patterns [1]. The underlying assumption of NMF*k* is that there are similar distributions of variables across samples such that the main characteristics of each sample can be represented by the combination of a limited number of non-negative additive components (signatures) [2]. It has also been widely used in environmental forensics [3, 4], text mining [5], face recognition [6]. Vesselinov et al. used NMF*k* to identify unknown recharge sources of groundwater driven by various physical and chemical processes [7]. Cai et al. used NMF to extract key features and reveal temporal changes in microbial communities [8]. Instead of linear transformation of the original dataset by correlations like principal components analysis (PCA), NMF*k* uses non-negativity constraints that makes it better suited to identify representative SOM signatures and evaluate their distribution in different samples. Furthermore, the additive fashion of extracted signatures by different weights in NMF*k* fit the intuition of different pools of SOM molecules combined into the mixture of SOM in a certain sample. Therefore, the NMF*k* extracted SOM signatures are more explainable compared to PCA or other ordination techniques.

The number of dominant types (k) was determined by silhouette coefficient with a threshold of 0.5 to test model stability [9, 10]. The last model above the threshold (> 0.5) is selected as the final model. This is because the selected model should have good separation between different non-negative signatures but also a stable solution at the same time.

Gradient Boosting regression models

Gradient boosting is a machine learning algorithm that combines multiple weak models, such as decision trees, into a stronger model iteratively, where each weak model learns from the residual error from the previous model.[11] It is one of the most powerful and effective machine learning models that is widely used in many different areas. Gradient boosting regression is an ensemble model that iteratively learns from the error of previous model. Using ensemble, it is capable to generate predictions from multiple decision tree models and thus provide a more robust prediction. It usually has better performance with smaller dataset, because it tends less overfit the data [12]. Therefore, it is suitable for predicting soil respiration with physicochemistry and SOM types.

We performed feature selection for physicochemical factors by statistical relevance (Table S1), to remove irrelevant features that likely introduce noise and leads to overfitting of the model.[13, 14] Total C, total N, CEC, Mn and soil moisture were selected as predictors for surface soil models. Total C, total N, total base, CEC, Mg and soil moisture were selected for subsoil models. The detailed settings of hyperparameter dictionary for *RandomizedSearchCV* function and the tunned parameter set used for the final model is in Table S2. To avoid the impacts of the increased number of predictors on improved model performance for surface respiration model (physicochemistry model: n = 5, SOM model: n = 7), we developed another version of SOM model without the two least important predictors (NMF7, NMF4). The model performance was still better (testing R^2 = 0.48 vs. 0.44) compared to the physicochemistry model with the same number of predictors (n = 5).

Supporting Tables

Table S1. Coefficient of Determination between soil respiration and soil biogeochemistry (Pearson's correlation R-square)

	Surface R^2	Surface p-value	Subsoil R^2	Subsoil p-value
Mn	**0.324**	**0.000**	**0.142**	**0.003**
Mg	**0.160**	**0.001**	**0.287**	**0.000**
K	0.004	0.638	0.053	0.071
Na	0.005	0.577	0.026	0.211
B	**0.119**	**0.006**	0.018	0.295
Zn	**0.173**	**0.001**	**0.102**	**0.011**
Fe	**0.089**	**0.017**	0.043	0.106
Cu	**0.092**	**0.016**	**0.133**	**0.004**
Total Base	**0.146**	**0.002**	**0.227**	**0.000**
CEC	**0.405**	**0.000**	**0.354**	**0.000**
Total C	**0.487**	**0.000**	**0.268**	**0.000**
Total N	**0.439**	**0.000**	**0.248**	**0.000**
Total S	**0.080**	**0.028**	0.036	0.160
GWC	**0.246**	**0.000**	**0.225**	**0.000**
Soil T	0.007	0.545	0.000	0.919
pH	**0.116**	**0.004**	0.007	0.513
SO4	**0.172**	**0.001**	0.002	0.759
P	0.001	0.855	0.003	0.695
NH4	0.002	0.761	0.000	0.992
NO3	0.004	0.634	0.004	0.634

Sand%	**0.140**	**0.001**	**0.176**	**0.000**
Silt%	**0.081**	**0.017**	**0.077**	**0.022**
Clay%	**0.157**	**0.001**	**0.182**	**0.000**
Elevation	**0.136**	**0.006**	**0.090**	**0.029**
alpha_div	**0.159**	**0.001**	**0.143**	**0.003**

Table S2. Hyperparameter tunning settings and the tunned hyperparameters used in each model.

Hyperparameter name	param_distributions	Physicochemistry Model		SOM Model		Physicochemistry & SOM Model	
		Surface	Subsoil	Surface	subsoil	surface	subsoil
n_estimators	randint(50,5000)	1213	1722	422	636	1392	351
max_depth	randint(2,60)	31	58	14	7	40	16
max_features	randint(1, X.shape[1])	1	6	2	5	3	7
min_samples_split	randint(2, 10)	6	6	4	6	7	9
learning_rate	[0.0001, 0.001, 0.01, 0.1, 1.0]	0.01	0.01	0.1	0.001	0.1	0.1
ccp_alpha	expon(scale=0.1)	0.0009419401	0.0173195734	0.0435524849	0.001778767	1.86731365e-05	0.000659532

Supporting Figures

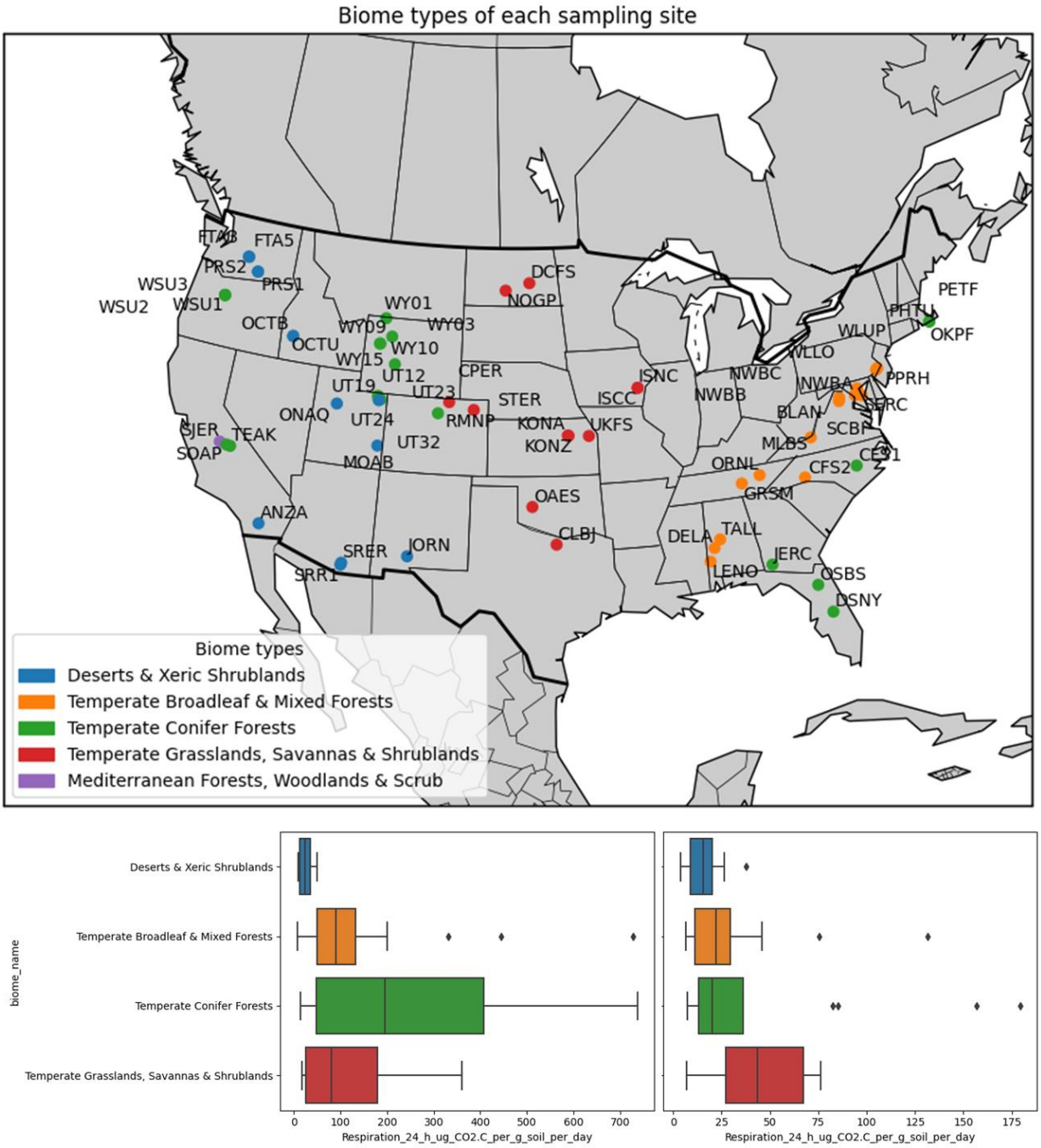

Figure S1. Sampling locations, sample names, and their biome types obtained from WWF terrestrial ecoregions (a). Difference of soil potential respiration by biomes in b) surface and c) subsoil.

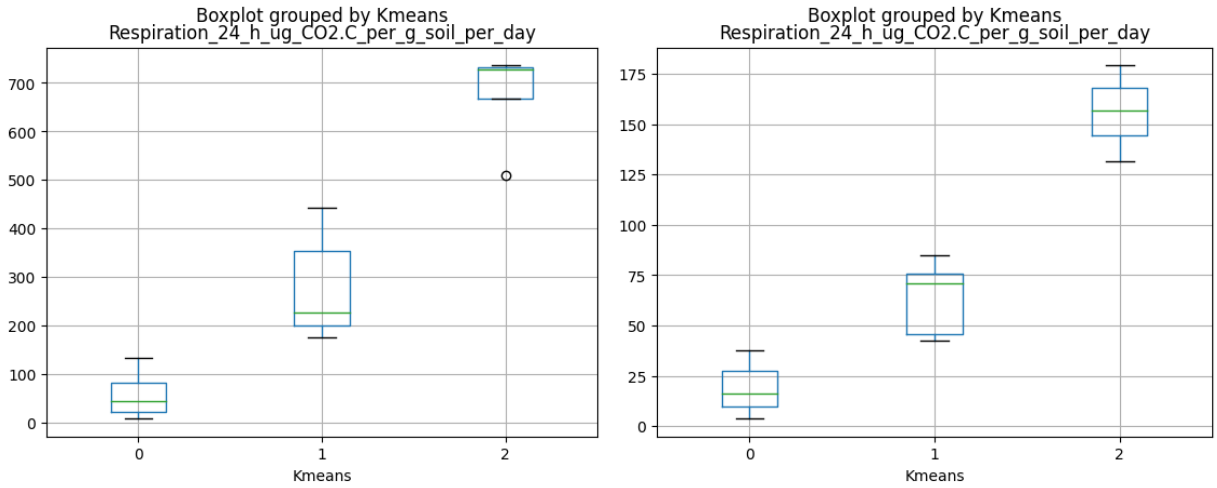

Figure S2. k-means clustering of soil respiration rates at different depths (a: surface soils, b: subsoils). 3 levels of respiration were determined for both surface and subsoil.

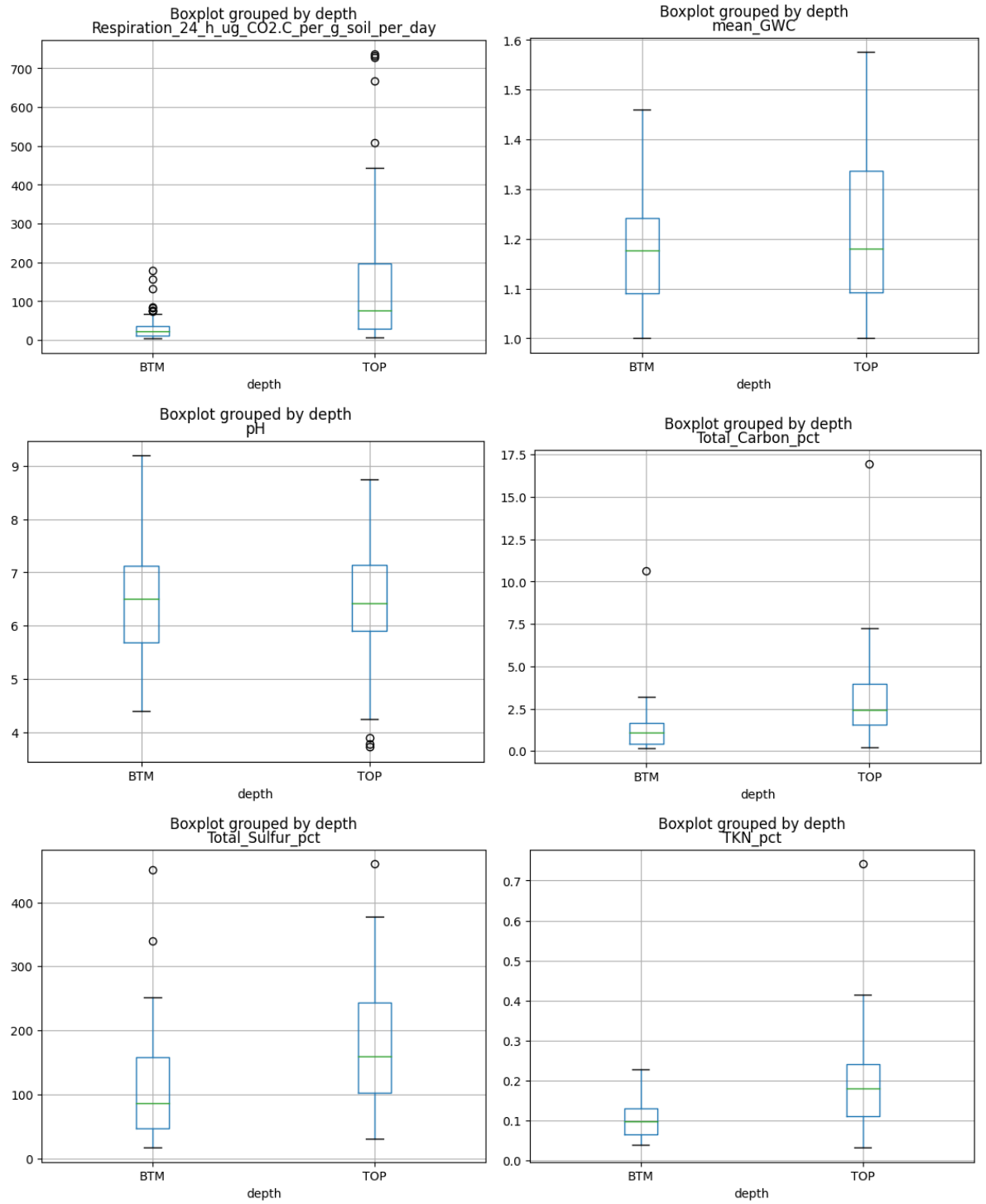

Figure S3. Boxplots of difference in soil biogeochemistry between surface and subsoils. a) potential respiration, b) moisture content, c) pH, d) total C, e) total S, f) total N.

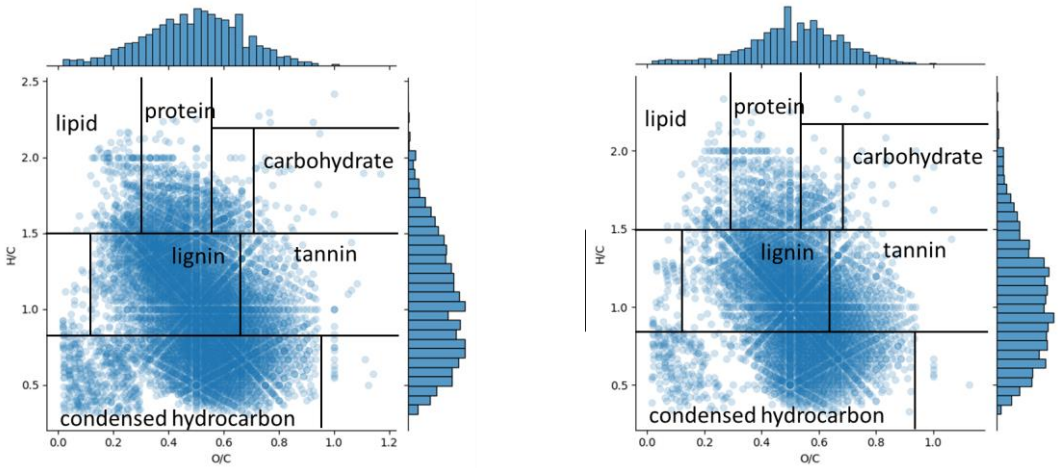

Figure S4 Van Krevelen Diagram of SOM formula identified in a) surface b) subsoils.

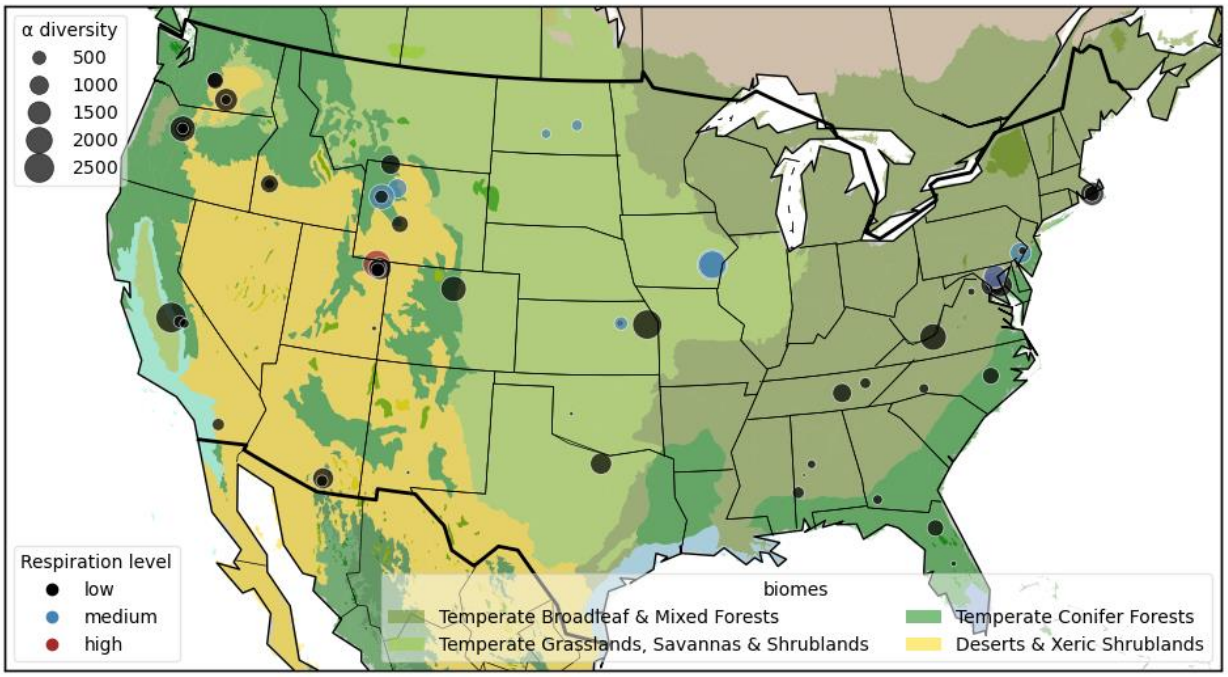

Figure S5. Spatial distribution of subsoil respiration levels (labeled by colors) and alpha diversity of each sample (sizes). Soil respiration levels are determined by K-means clustering on soil respiration rates (ug CO2/g soil/day)

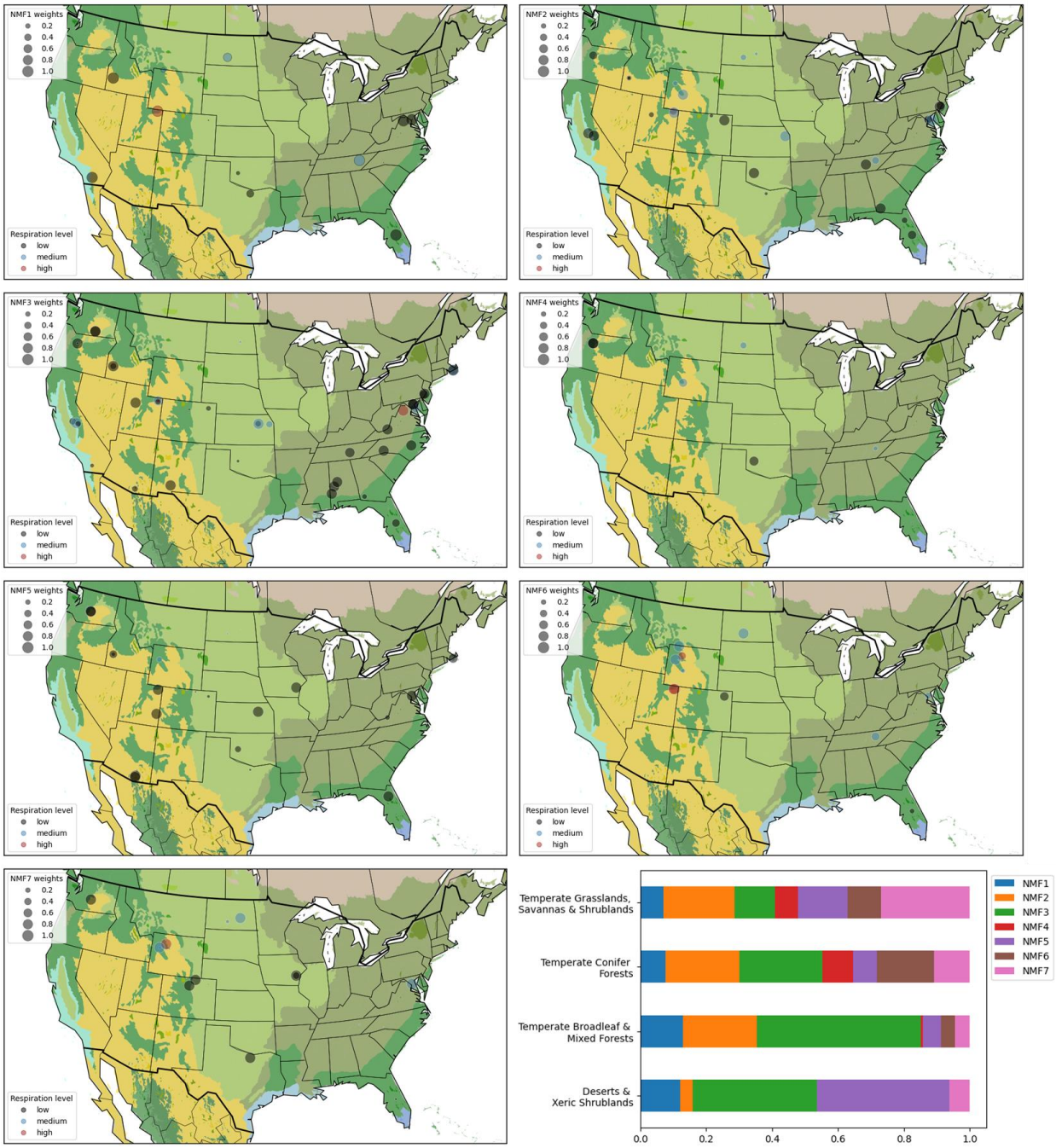

Figure S6. The weights of 7 surface soil SOM types in all samples identified by NMF*k* using SOM composition data obtained from FT-ICR MS, and the relative contribution of the 7 types in each biome. Deserts & Xeric Shrublands (N = 13), Temperate Broadleaf & Mixed Forests (N = 17), Temperate Conifer Forests (N = 21), Temperate Grasslands, Savannas & Shrublands (N = 11).

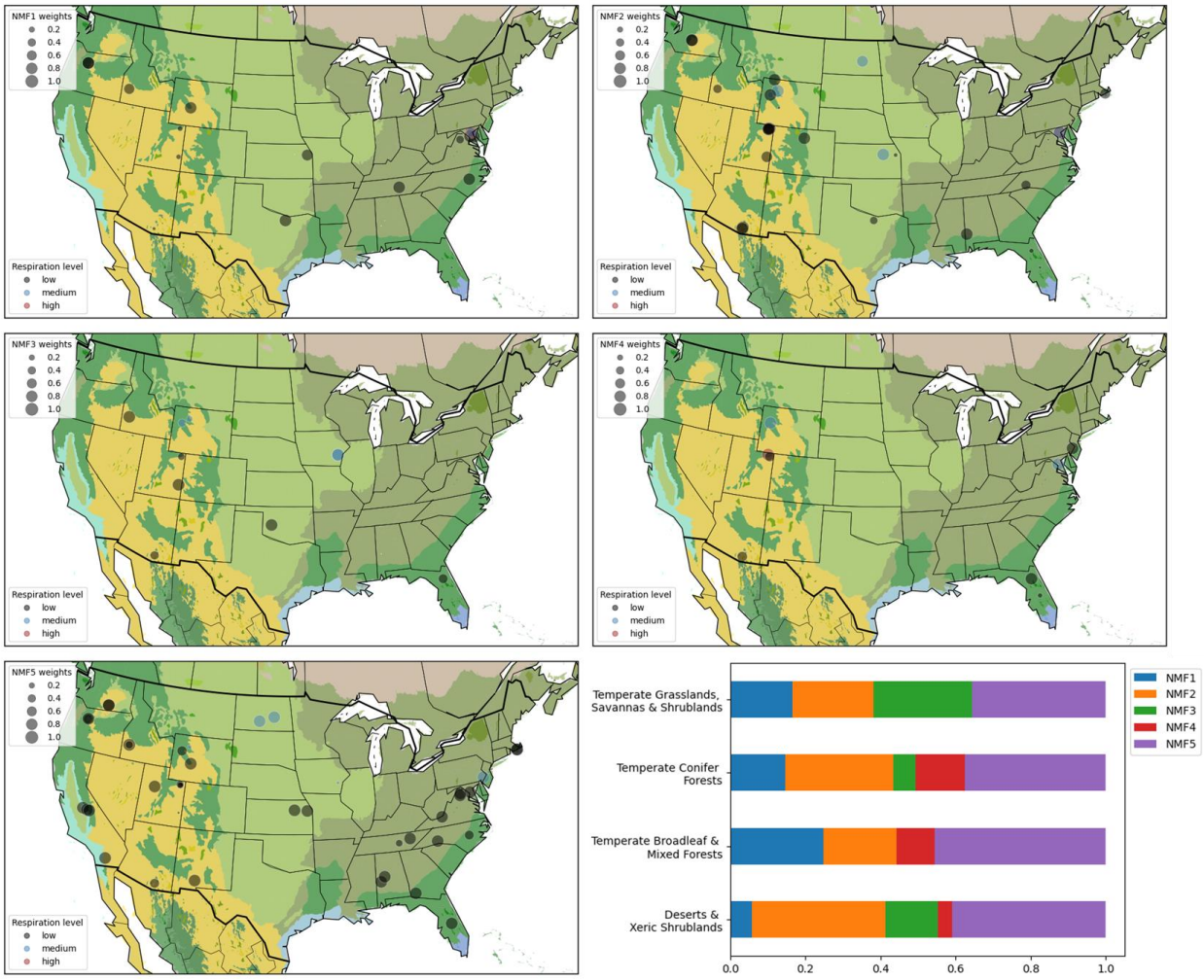

Figure S7. The weights of 5 subsoil SOM types in all samples identified by NMF*k* using SOM composition data obtained from FT-ICR MS, and the relative contribution of the 5 types in each biome. Deserts & Xeric Shrublands (N = 13), Temperate Broadleaf & Mixed Forests (N = 17), Temperate Conifer Forests (N = 21), Temperate Grasslands, Savannas & Shrublands (N = 9).

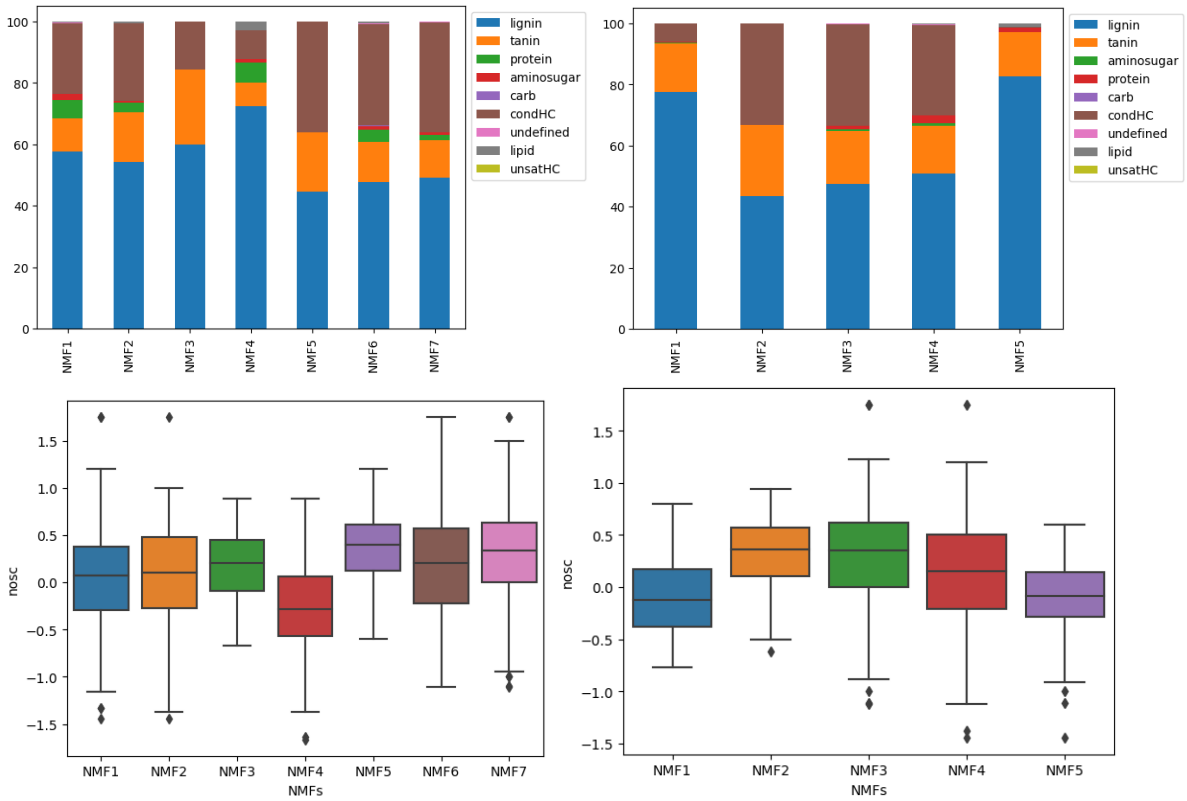

Figure S8. Relative contribution of each compound class to each NMF type for important features with normalized weights of greater than 0.5 in a) surface soil and b) subsoil. Boxplot shows the difference of Nominal Oxidation State of Carbon (NOSC) Values for the important compounds (w > 0.5) for each NMF in c) surface soil and d) subsoil.

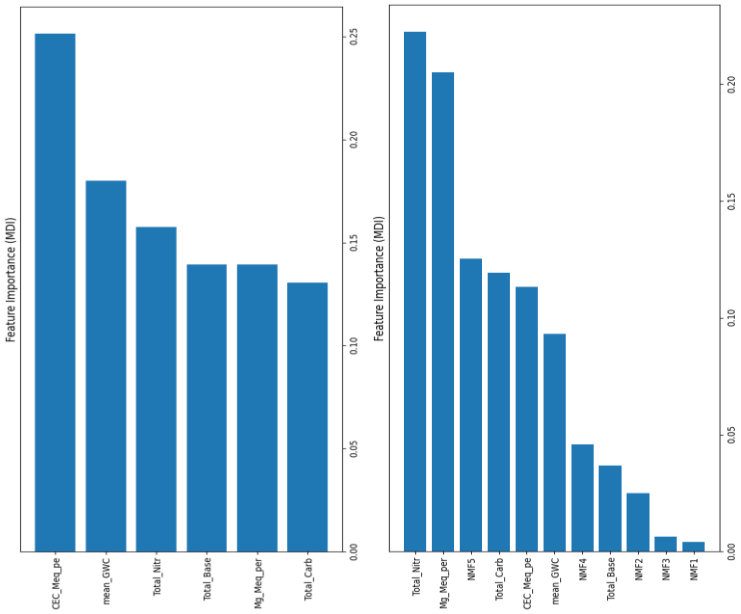

Figure S9. Relative importance of each predictor in subsoil potential respiration models. a) Physicochemical model, with biogeochemical variables only. b) Physicochemistry &SOM_model with both physicochemical variables and SOM types. (SOM model for subsoil has bad performance (Table 1) and therefore feature importance is not reported here).

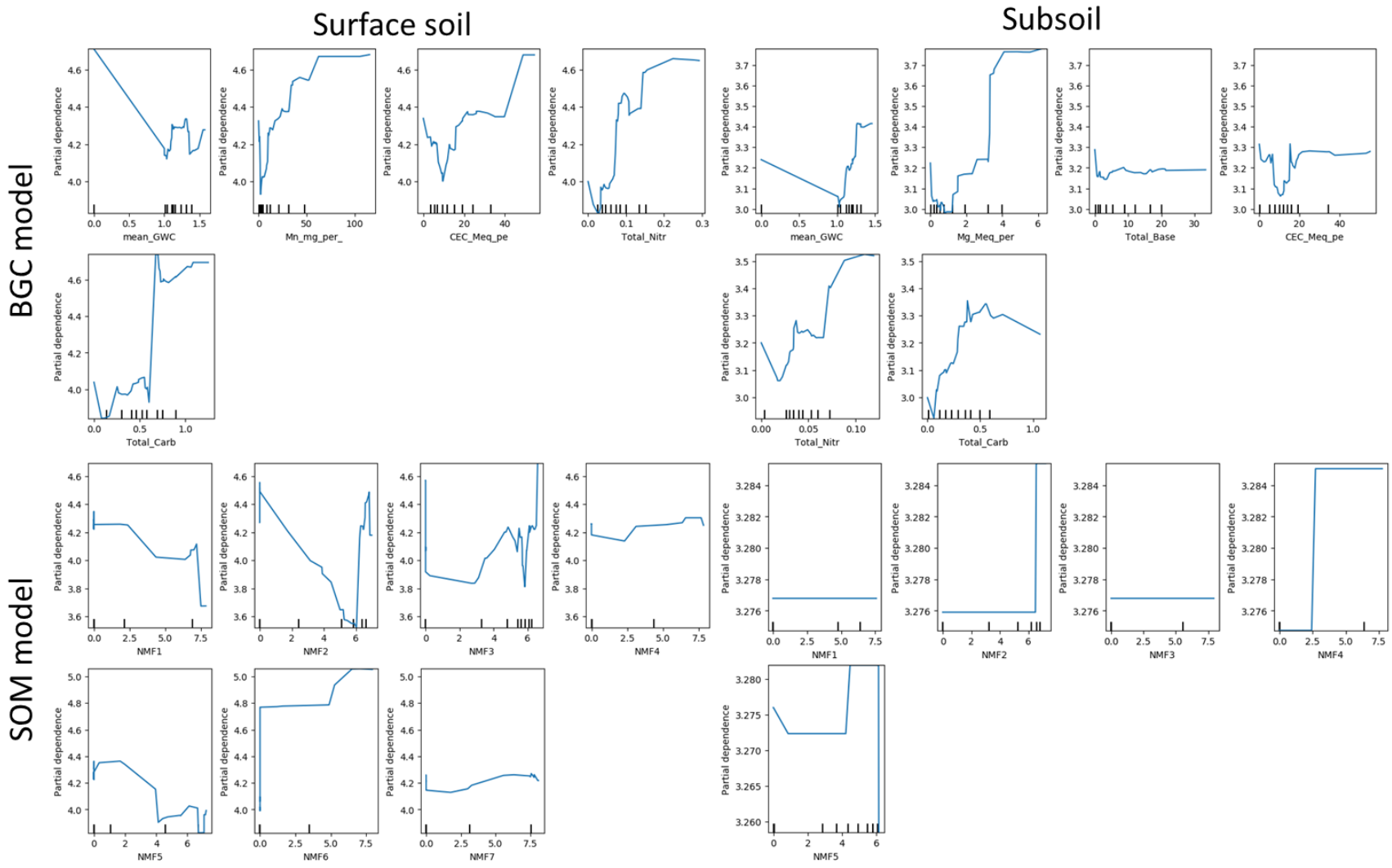
Surface soil
Subsoil
BGC model
SOM model
Partial dependence
mean_GWC
Mn_mg_per_
CEC_Meq_pe
Total_Nitr
Total_Carb
Mg_Meq_per
Total_Base
NMF1
NMF2
NMF3
NMF4
NMF5
NMF6
NMF7

BGC&SOM model

Surface soil

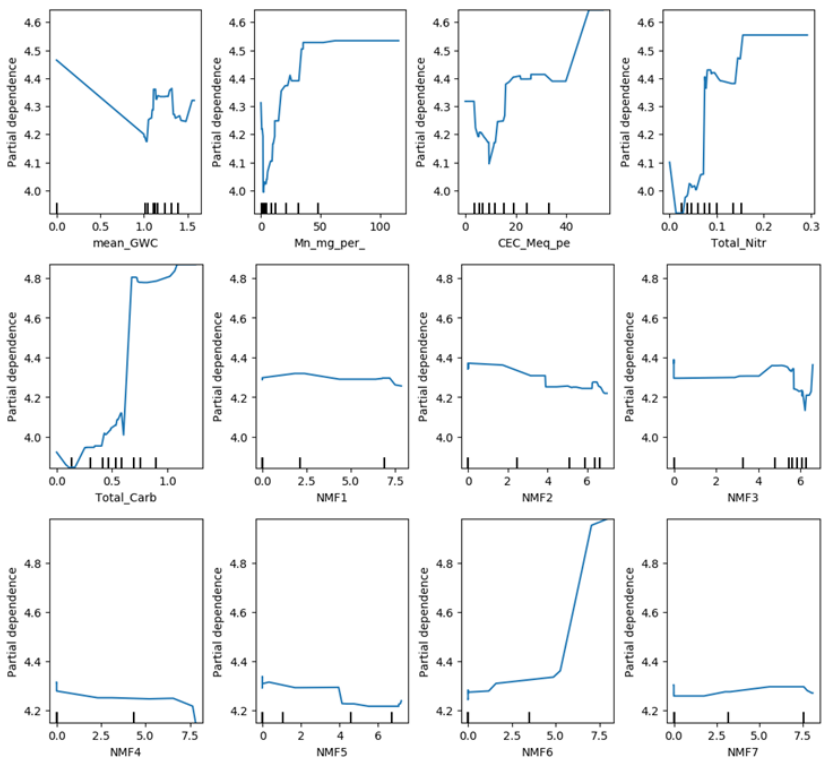

Subsoil

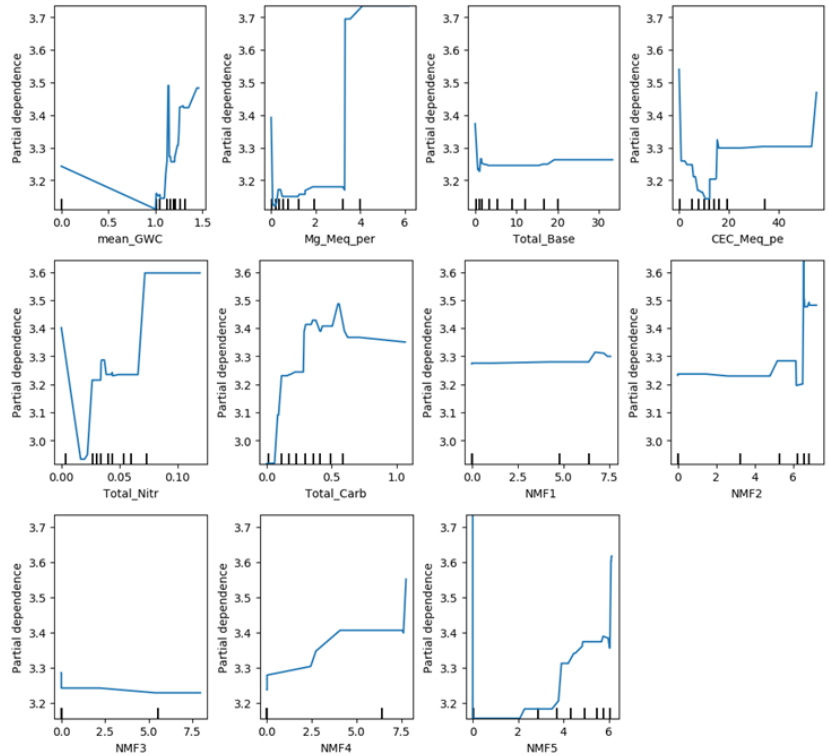

Figure S10. Partial dependence of potential respiration to predictors of soil biogeochemistry and/or SOM composition in surface and subsoil models. a) BGC model with biogeochemical variables for surface soil, b) BGC model with biogeochemical variables for subsoi,l c) SOM model with SOM variables for surface soil, d) SOM model with SOM variables for subsoil (bad model performance), e) BGC&SOM model with both biogeochemical and SOM variables for surface soil, f) BGC&SOM model with both biogeochemical and SOM variables for subsoil.

References

1. Lee, D.; Seung, H. S., Algorithms for non-negative matrix factorization. *Advances in neural information processing systems* **2000,** *13*.
2. Paatero, P.; Tapper, U., Positive matrix factorization: A non-negative factor model with optimal utilization of error estimates of data values. *Environmetrics* **1994,** *5*, (2), 111-126.
3. Johnson, G. W.; Ehrlich, R.; Full, W.; Ramos, S., Principal components analysis and receptor models in environmental forensics. In *Introduction to environmental forensics*, Elsevier: 2015; pp 609-653.
4. Rodenburg, L. A.; Du, S.; Xiao, B.; Fennell, D. E., Source apportionment of polychlorinated biphenyls in the New York/New Jersey Harbor. *Chemosphere* **2011,** *83*, (6), 792-798.
5. Pauca, V. P.; Shahnaz, F.; Berry, M. W.; Plemmons, R. J. In *Text mining using non-negative matrix factorizations*, Proceedings of the 2004 SIAM international conference on data mining, 2004; SIAM: 2004; pp 452-456.
6. Guillamet, D.; Vitria, J. In *Non-negative matrix factorization for face recognition*, Catalonian Conference on Artificial Intelligence, 2002; Springer: 2002; pp 336-344.
7. Vesselinov, V. V.; Alexandrov, B. S.; O'Malley, D., Contaminant source identification using semi-supervised machine learning. *Journal of Contaminant Hydrology* **2018,** *212*, 134-142.
8. Cai, Y.; Gu, H.; Kenney, T., Learning Microbial Community Structures with Supervised and Unsupervised Non-negative Matrix Factorization. *Microbiome* **2017,** *5*, (1), 110.
9. Vangara, R.; Bhattarai, M.; Skau, E.; Chennupati, G.; Djidjev, H.; Tierney, T.; Smith, J. P.; Stanev, V. G.; Alexandrov, B. S., Finding the Number of Latent Topics With Semantic Non-Negative Matrix Factorization. *IEEE Access* **2021,** *9*, 117217-117231.
10. Bhattarai, M.; Chennupati, G.; Skau, E.; Vangara, R.; Djidjev, H.; Alexandrov, B. S. In *Distributed Non-Negative Tensor Train Decomposition*, 2020 IEEE High Performance Extreme Computing Conference (HPEC), 22-24 Sept. 2020, 2020; 2020; pp 1-10.
11. Friedman, J. H., Greedy function approximation: a gradient boosting machine. *Annals of statistics* **2001**, 1189-1232.
12. Hastie, T.; Tibshirani, R.; Friedman, J. H.; Friedman, J. H., *The elements of statistical learning: data mining, inference, and prediction*. Springer: 2009; Vol. 2.
13. Christ, M.; Braun, N.; Neuffer, J.; Kempa-Liehr, A. W., Time Series FeatuRe Extraction on basis of Scalable Hypothesis tests (tsfresh – A Python package). *Neurocomputing* **2018,** *307*, 72-77.
14. Yuan, B.; Tan, Y. J.; Mudunuru, M. K.; Marcillo, O. E.; Delorey, A. A.; Roberts, P. M.; Webster, J. D.; Gammans, C. N. L.; Karra, S.; Guthrie, G. D.; Johnson, P. A., Using Machine Learning to Discern Eruption in Noisy Environments: A Case Study Using CO2-Driven Cold-Water Geyser in Chimayó, New Mexico. *Seismological Research Letters* **2019,** *90*, (2A), 591-603.